MODELLING EFFECTS OF INSUFFICIENT LAP SPLICES ON A DEFICIENT REINFORCED CONCRETE FRAME

A THESIS SUBMITTED TO
THE GRADUATE SCHOOL OF NATURAL AND APPLIED SCIENCES
OF
MIDDLE EAST TECHNICAL UNIVERSITY

BY

WESLEY WEI-CHIH LIN

IN PARTIAL FULFILLMENT OF THE REQUIREMENTS
FOR
THE DEGREE OF MASTER OF SCIENCE
IN
EARTHQUAKE ENGINEERING AND ENGINEERING SEISMOLOGY

JANUARY 2013

Approval of the thesis:

MODELLING EFFECTS OF INSUFFICIENT LAP SPLICES ON A DEFICIENT REINFORCED CONCRETE FRAME

submitted by **WESLEY WEI-CHIH LIN** in partial fulfillment of the requirements for the degree of **Master of Science in Earthquake Engineering and Engineering Seismology, Middle East Technical University** by,

Prof. Dr. Canan Özgen _____
Dean, Graduate School of **Natural and Applied Sciences**

Prof. Dr. Ahmet Cevdet Yalçıner _____
Head of Department, **Civil Engineering**

Prof. Dr. Haluk Sucuoğlu _____
Supervisor, **Civil Engineering Dept., METU**

Prof. Dr. Barış Binici _____
Co-Supervisor, **Civil Engineering Dept., METU**

Examining Committee Members:

Prof. Dr. Güney Özcebe _____
Civil Engineering Dept., METU

Prof. Dr. Haluk Sucuoğlu _____
Civil Engineering Dept., METU

Prof. Dr. Ahmet Yakut _____
Civil Engineering Dept., METU

Assoc. Prof. Dr. Erdem Canbay _____
Civil Engineering Dept., METU

Asst. Prof. Dr. Tahsin Turgay _____
Architecture Dept., Abant İzzet Baysal University

Date: 29.01.2013

I hereby declare that all information in this document has been obtained and presented in accordance with academic rules and ethical conduct. I also declare that, as required by these rules and conduct, I have fully cited and referenced all material and results that are not original to this work.

Name, Last name: Wesley Wei-Chih Lin

Signature : _____

ABSTRACT

MODELLING EFFECTS OF INSUFFICIENT LAP SPLICES ON A DEFICIENT REINFORCED CONCRETE FRAME

Lin, Wesley Wei-Chih
M.Sc., Department of Civil Engineering
Supervisor: Prof. Dr. Haluk Sucuoğlu
Co-Supervisor: Prof. Dr. Barış Binici

January 2013, 63 pages

In order to reduce seismic risk in vulnerable buildings, buildings identified to be at risk should be assessed and strengthened. Performance evaluation of deficient buildings has become a major concern due to devastating earthquakes in the past. In order to justify new provisions in design and assessment codes, experiments and analyses are inherently necessary.

In this thesis study, investigations into the behaviour of two deficient reinforced concrete frames built at Middle East Technical University's Structural and Earthquake Laboratory and tested via pseudo-dynamic tests were made. These frames were modelled on the OpenSees platform by following methods of analyses outlined in the Turkish Earthquake Code of 2007 (TEC 2007) and ASCE/SEI-41-06. Both deficient frames were essentially the same, with the only difference being the presence of insufficient lap splices, which was the focus of the study.

Time history performance assessments were conducted in accordance to TEC 2007's damage state limits and ASCE/SEI 41-06's performance limits. The damages observed matched the performance levels estimated through the procedure outlined in TEC 2007 rather well. Specific to the specimen with lap splice deficiencies, ASCE/SEI 41-06 was overly conservative in its assessments.

TEC 2007's requirements for lap splice lengths were found to be conservative in the laboratory and are able to tolerate deficiencies up to 25% of the required length.

With respect to mathematical models, accounting for materials in deficient systems by using nominal but reduced strength properties is not very efficient and unless joint deformations are explicitly accounted for, local deformations cannot be captured.

Keywords: Pseudo-Dynamic Testing, Numerical Simulations, Performance Evaluations, Lap Splice Deficiencies

ÖZ

YÖNETMELİĞE UYGUN OLMAYAN BETONARME ÇERÇEVEDE YETERSİZ BİNDİRMELİ EKLERİN MODELLEMEDEKİ ETKİLERİ

Lin, Wesley Wei-Chih
Yüksek Lisans, İnşaat Mühendisliği Bölümü
Tez Yöneticisi: Prof. Dr. Haluk Sucuoğlu
Ortak Tez Yöneticisi: Prof. Dr. Barış Binici

Ocak 2013, 63 sayfa

Hasar almaya yatkın binalardaki sismik tehlikeyi azaltmak için, riskli olduğu belirlenen binalar değerlendirilmeli ve güçlendirilmelidir. Zayıf binaların performans değerlendirmesi geçmişteki yıkıcı depremler nedeniyle önemli bir mesele haline gelmiştir. Tasarım ve değerlendirme yönetmeliklerindeki yeni koşulları doğrulamak için deney ve analiz yapmak gereklidir.

Bu çalışmada, Orta Doğu Teknik Üniversitesi Yapı ve Deprem Laboratuvarı'nda inşa edilmiş ve dinamik benzeri deney yöntemi ile test edilmiş yönetmeliğe uygun olmayan iki betonarme çerçevenin davranışı incelenmiştir. Söz konusu çerçeveler Deprem Bölgelerinde Yapılan Binalar Hakkında Yönetmelik (DBYBHY 2007) ve ASCE/SEI 41-06'da belirtilen metodlar takip edilerek OpenSees platformunda modellenmiştir. Bu çalışmanın odak notkası olan yetersiz bindirmeli eklerin bir çerçevede bulunması haricinde, her iki yönetmeliğe uygun olmayan çerçeve de aslen aynıdır.

Zaman tanım alanında hesap yöntemi ile performans değerlendirmeleri DBYBHY 2007 ve ASCE/SEI 41-06'nın performans limitlerine göre yapılmıştır. Gözlemlenen hasarlar DBHBHY 2007'de belirtilen prosedürle hesaplananan performans seviyelerile iyi bir şekilde örtüşmüştür. Bindirmeli ek yetersizliği olan numune için ASCE/SEI 41-06 değerlendirmede fazla güvenli sonuç vermiştir.

DBHBHY 2007'nin bindirmeli ek boyu ile ilgili koşullarının fazla güvenli olduğu laboratuvarda bulunmuş ve mevcut gerekli uzunluğun %25'ine kadar yetersizliğin tolere edilebildiği gözlemlenmiştir.

Matematiksel modellere göre, yönetmeliğe uygun olmayan sistemlerde malzeme dayanım özelliklerinin nominal değerlerin azaltılmışlarını kullanmak çok etkili değildir. Ayrıca, kolon-kiriş birleşim bölgesi deformasyonları açık bir şekilde hesaba katılmadığı sürece lokal deformansyonlar yakalanamamaktadır.

Anahtar Kelimeler: Dinamik Benzeri Test Yöntemleri, Numerik Simulasyonlar, Performans Değerlendirmesi, Bindirmeli Ek Yetersizlikleri

ACKNOWLEDGEMENTS

It would not have been possible to write this thesis without the help and support of the people in my life. There are too many to mention everyone by name; if I thanked them all, the acknowledgements would be longer than my thesis! Above all, I would like to thank my mother, Mei-Mei Cheng, who has encouraged and supported me my whole life. I am forever indebted to my father, Oscar Po-Hsiu Lin, for his decision to immigrate to Canada in pursuit of a better life for his family, May he rest in peace. To my sisters Milly and Tina, my thanks for their understanding on the various decisions I have made and will make in my life.

This thesis would not have been possible without the guidance and direction of my principal supervisor, Dr. Haluk Sucuoğlu, and my co-supervisor, Dr. Barış Binici at the Middle East Technical University. I thank the following professors at the University of British Columbia, in chronological order, who encouraged me to pursue a career in academia: Dr. Reza Vaziri, Dr. Siegfried Stiemer, and Dr. Kenneth Elwood.

To my friends in the simulations laboratory, I am grateful for the various forms of support you have provided me. To Umair Ahmed Siddiqui, you will always be my "yar".

I would like to acknowledge the financial support of the European Commission under the scope of its Erasmus Mundus programme, and the Scientific and Technological Research Council of Turkey (Tübitak), both of which provided the necessary funds that enabled me to pursue my Masters degree abroad.

For any errors or inadequacies that may remain in this work, the responsibility is entirely my own.

TABLE OF CONTENTS

LIST OF TABLES

TABLES

LIST OF FIGURES

FIGURES

CHAPTERS

1. INTRODUCTION

1.1 General

Many reinforced concrete buildings around the world are insufficiently designed and/or constructed, according to modern seismic codes, regulations, and best practices. In order to reduce seismic risk in vulnerable buildings, buildings identified to be at risk should be assessed and strengthened. In recent history, there has been an absence of technical standards for risk reduction processes.

Performance evaluation of deficient buildings has become a major concern due to recent devastating earthquakes in Turkey which caused significant economic and human loss. Preliminary seismic performance assessments funded by the government of Turkey had revealed that a significant number of buildings have numerous deficiencies. The most observed deficiencies are as follows: plan irregularities, presence of heavy overhangs, poor detailing in structural members and joint regions, low material strengths, inadequate member sizes and finally, the use of plain reinforcements, which is of particular interest to this study. Buildings constructed before the 1980s had splices which were designed for compression only, leading to insufficient development lengths in tension.

Different deficiencies have various local and global effects on the seismic performance of buildings and should thus be studied separately. Proper rehabilitation of existing buildings before a major earthquake hits is of utmost importance, as many populated cities in Turkey are located in high seismic zones.

To the best of the author's knowledge, the effect of lap splice deficiencies have mostly been examined in the literature via individual column tests, such as the tests conducted by Aboutaha et al. (1996), Lynn et al. (1996), Melek and Wallace (2004), and Eshghi and Zanjanizadeh (2007). There are a limited number of frame tests investigating the behaviour of columns with insufficient splice lengths, such as the tests conducted by Canbay (2003) and Akin (2011). However, frame test with such deficiencies tested under realistic earthquake demands are scarce. Thus, the opportunity to examine lap splice deficiencies and their local and global effects on reinforced concrete frames subjected to earthquake ground motions would greatly benefit the engineering community.

Released in 1997, FEMA 273 (Guidelines for the Seismic Rehabilitation of Buildings) was one of the leading global comprehensive documents which proposed various technical requirements for the seismic rehabilitation of existing buildings. Soon after, in 2000, FEMA 356 (Prestandard and Commentary for the Seismic Rehabilitation of Buildings) replaced FEMA 273 and became the new benchmark document. Methods outlined in FEMA 356 served as a basis for future developments and research topics of many codes and regulations around the globe. As this document was revised and improved over time, it was replaced by ASCE/SEI 41-06 (Seismic Rehabilitation of Existing Buildings) in 2006. In 2007, a document titled ASCE/SEI 41 Supplement-1, based on research on the proposed effective stiffness models, modeling parameters, and acceptance criteria, was released. This supplement to the original ASCE/SEI 41 contained provisions related to the rehabilitation of existing reinforced concrete buildings. ASCE/SEI 41-13 is scheduled to be released in 2013, but there are virtually no changes for the reinforced concrete provisions outlined in the first supplement.

The current seismic building code in Turkey, the Turkish Earthquake Code 2007 (TEC 2007), was released in 2007 and provides evaluation methods and performance limits for use in building design. The procedures outlined in TEC 2007 are similar to those of ASCE/SEI 41-06. However, for the first time in design code history, the Ministry of Construction and Resettlement in Turkey added a section

regarding the assessment and strengthening of existing buildings to TEC 2007 in 2007, employing a performance-based vision. The procedures outlined in TEC 2007 need detailed verification studies, as they slightly differ from the point defining the member acceptance criteria. Leading earthquake engineering countries such as the USA and Japan do not have legal documents regarding this matter and thus renders comparative analyses impossible. As mentioned before, Turkey is in an urgent situation in terms of the amount of seismic rehabilitation needed in the country. Thus, research on the reliability of these proposed methods is essential for future revisions and improvements on the current code.

1.2 Analyses Methods

There are two main groups of analysis procedures which are deemed acceptable in the engineering community for the estimation of seismic demands of structures: Response spectrum and dynamic analyses. Static and dynamic analyses can both be linear or nonlinear, each varying in computational effort and accuracy.

Static analysis methods estimate the dynamic ground motion input response through statistical modal combination rules, which inherently introduce errors into the analysis since directional combination of the modal responses is ignored. These errors are more prominent when estimating member forces as statistical combination rules generally predict a higher capacity. Using nonlinear static (pushover) analysis is often seen as an acceptable trade-off between accuracy and computational effort for low to mid-rise buildings, as it normally yields sufficiently accurate results for engineers. This procedure applies a lateral static force profile to the structure until the desired target displacement is reached. Within nonlinear static analysis, there are various ways to apply this force vector. The most conventional method is to use the first mode's force vector, obtained from the first mode shape of the structure through classical structural dynamics theory. This is an acceptable procedure for structures which are primarily first mode dominant, which is the case of the test specimens discussed in this thesis study. The inability of conventional nonlinear static analysis for capturing higher mode effects is recognized, and for structures which are not first-mode dominant, adaptive pushover analysis procedures were proposed by Chopra and Goel (2002). As discussed in a later section, the test specimens studied in this thesis are first-mode dominant. Therefore, higher mode effects are not expected.

Nonlinear dynamic (time history or response history) analysis procedure is accepted as the most accurate amongst all four types of analysis methods. However, this type of analysis requires the highest computational effort in terms of run time, computing power, and post-processing as it is the most complex method of all. Convergence and stability problems are the most common issues which arise, and are especially present in computer software. The sources of these errors are difficult to detect and solve.

This study will focus on nonlinear static and nonlinear dynamic analyses, with both methods being implemented on the OpenSees platform for the test specimens.

OpenSees is an acronym for Open System for Earthquake Engineering Simulation and is an object-oriented, open-source software created at the Pacific Earthquake Engineering Center. The program is used for finite element modelling in the simulation of the response of structural and geotechnical systems subjected to earthquakes. OpenSees is able to model and analyze the nonlinear static and dynamic response of systems using various material models, elements, and solution algorithms.

1.3 Seismic Assessment Models

During a ground excitation, lateral loads imposed by earthquakes on a conventional reinforced concrete frame are carried by the gravity load-bearing columns of the structure. Thus, these columns need to be adequately designed in order to have the sufficient strength and ductility required from the force and displacement demands of an earthquake. When designing a reinforced concrete structure, it is imperative that an estimation of column ductility be as accurate as possible, as this is one of the main governing factors of its seismic performance and failure mechanisms.

In performance-based assessments, individual structural members are classified according to their expected failure modes based on their nonlinear deformation capacities. These classifications are then used to determine modelling parameters and deformation limits for a pre-defined performance level.

In the original ASCE/SEI 41-06, provisions for modelling parameters and numerical acceptance criteria of reinforced concrete elements were not classified based on flexure failure, shear failure, shear/flexure failure, or inadequate lap splicing. It is stated in EERI/PEER (2006) that the original proposed acceptance criteria from ASCE/SEI 41-06 yield conservative results. Furthermore, a study conducted by Sezen and Moehle (2006) showed the existence of limited plastic deformation capacities of columns due to flexural yielding prior to shear failure, commonly known as the flexure-shear failure. Thus, a revision of ASCE/SEI 41-06's deformation limits was required in order to improve future estimations.

Classifications of columns for determining modelling parameters were revised and published in ASCE/SEI 41 Supplement-1, which included the flexure-shear failure mode. In this supplement, three conditions are defined and classification of columns is obtained through its shear capacity/demand ratio and the transverse reinforcements of critical sections. Once classified, modelling parameters and acceptance criteria can be obtained for each type of failure mode: flexure, flexure-shear, and shear. However, Acun and Sucuoglu (2010) suggested that the new deformation-based performance limits proposed for nonconforming columns were still conservative in setting the rotation limits of life safety and collapse prevention, which may yield misleading results in the seismic risk assessment of existing concrete structures. They noted that the performance limits also appeared to be very conservative in predicting the experimental performance of column plastic hinges designed to fail in pure flexure under moderate axial load levels.

In Chapter 7 ("Seismic Assessment and Retrofit Design of Existing Buildings") of TEC 2007, structural members are classified into either ductile or brittle failure, which correspond to flexure and shear failure as defined in FEMA 356, respectively. TEC 2007 has yet to include the flexure-shear mode in its classification procedures, which is essential in order to accurately estimate member modelling parameters and acceptance criteria.

It is essential in both linear and nonlinear modelling that joint strength and flexibility capacities are captured as accurately as possible. Earthquake-induced deformations in moment resisting frames cause moment reversals at beam-column joints which may induce high shear demands in these regions. Unless rigorously modelled, frame stiffness reduction and/or premature strength loss may not be captured correctly.

Before the onset of plasticity, the elastic portion of a beam-column joint behaviour can be modelled with rigid end offsets of various lengths to model the joint flexibility.

In FEMA 356, the simple approach of setting rigid end offsets equal to the joint dimensions is recommended. ASCE/SEI 41-06 refined this approach by defining rigid end offset lengths as a function of the flexural strength of connected beam-columns. In the case of a strong column-weak beam system, rigid offsets are only required for columns, whereas in a strong beam-weak column system, rigid offsets are only recommended for beams. For intermediate cases, half the length of the joint dimension is modelled as the rigid offset length for columns and beams at the joint. TEC 2007 states that full rigid offsets are defined for both the columns and beams.

In a recent study by Birely et al. (2012), recommended procedures from FEMA 356 and ASCE/SEI 41-06 for rigid offsets were evaluated in light of 45 experiments. The main findings were: i) defining rigid offsets as per FEMA 356 resulted in overly stiff models and using ASCE/SEI 41-06 resulted in more realistic values; ii) FEMA 356 predicts an overly stiff model which inaccurately predicts the initial yield displacements of experiments, while ASCE/SEI 41-06's predictions are generally good, except for in the case of joints which do not satisfy the requirements of ACI 318-08. Thus, it was recommended that an alternative definition of rigid offsets be set for joint compliance/non-compliance with ACI 318-08, in order to improve the estimation of initial yield displacements.

The behaviour of beam-column joints has been an extensive researched topic in the past, resulting in the general conclusion that joints may experience high shear deformations prior to the yielding of longitudinal reinforcement. Once beam-column joints enter the plastic region, proper modelling of their nonlinear behaviour becomes an important factor in accurate simulations.

1.4 Modelling Deficient Lap Splices

The strength from steel reinforcement in concrete is primarily achieved through two mechanisms: mechanical interlock between the concrete and reinforcing steel (only in deformed rebar), and frictional strength due to the cement chemical bond. Since the specimens of interest in this dissertation only contain plain reinforcing steel, strength is only developed due to friction achieved by chemical bonds**.**

In order to ensure proper strength development in reinforcement, proper control of sufficient bar spacing/cover, use of transverse reinforcement, and minimizing bar sizes are needed. In most design codes, the development length is a function of:

- The rebar diameter;
- The concrete strength/density;
- The concrete cover;
- The steel strength;
- The location of the rebar in beams (top or bottom)
- The quality of the bond due to vibration; and
- The presence of epoxy coating

It is of interest to understand the effects of inadequate lap splices because structures with such deficiencies exist all around the world, and a reliable method in assessing and strengthening buildings would greatly benefit the engineering community. Inadequate lap splices in a structure often result in premature failure which in turn leads to injuries and/or casualties in the event of an earthquake.

A structure's strength and deformation response are highly affected by the lap splice length. Insufficient ductility of a structure arises from insufficient transverse reinforcement (due to insufficient confinement) and insufficient lap splices in the plastic hinge zone.

When design provisions of a building code are not met, the deficiencies greatly diminish its capacity. In seismic assessment, guidelines usually do not require each of these deficiencies be modelled on a local scale, but recommend implicit methods to account for their effects.

The following list summarizes various research teams which have proposed formulae for determining the bond strength between lap-spliced reinforcement and concrete:

- Orangun et al. (1977) – considered concrete cover, bar diameter, lap-splice length, material properties, and amount of transverse reinforcement;
- Eligehausen et al. (1983) – considered unconfined and well-confined concrete and proposed a model which includes ascending, yielding, softening, and a final constant stress zone;
- Soroushian et al. (1991) – considered effects of confinement and concrete strength on local slip conditions of deformed bars;
- Xu (1992) – considered bond strength through experimental statistical regression and stress-state analysis;
- Harajli (1994) – considered reinforcement in plain and fibre-reinforced concrete
- Priestley et al. (1996) – considered fracture mechanics;
- Xiao et al. (1997) – considered modifications to pre-existing ACI definitions;
- Ghobarah et al. (2003) – considered the effect of bar slip on the flexural strength of columns;
- Sezen et al. (2003) – considered the effect of bar slip on deformations with a focus on rigid body rotations due to bar elongation and slip in the joints (strain penetration effect);
- Zhao et al. (2006) – proposed a zero length element capable of modelling the strain penetration effect

As suggested in TEC 2007 and ASCE/SEI 41-06, joint/lap splice deficiencies in mathematical models are indirectly accounted for through a reduction factor of steel yield strength. In the case of TEC 2007, this factor is a linear reduction in proportion to the splice length to development length ratio, whereas the factor in ASCE/SEI-41-06 is an exponential factor of the same ratio. The presence of insufficient lap splice lengths that decrease a structure's capacity in analyses is based on various experimental results.

1.5 Objectives and Scope

In order to justify new provisions in design and assessment codes, experiments and analyses are inherently necessary. This ensures that modelling parameters are adequate enough for accurate seismic assessment and rehabilitation of existing structures. The Scientific and Technological Research Council of Turkey (Tübitak) funded a research project at Middle East Technical University (METU)'s Structural and Earthquake Laboratory for the verification and validation of the existing assessment and performance-based design methodologies in TEC 2007 through analyzing and testing various concrete frames.

The project is titled: "Developing Performance-Based Evaluation Procedures and Strengthening Methods for the Turkish Seismic Code through Experimental and Analytical Research" and is officially documented as "TÜBİTAK 1007, Project #108G034".

The project has a duration of 36 months and commenced on February 15, 2010. This thesis investigates the behaviour of test specimens, Specimen #5 (hereinafter referred to as Specimen #1) and Specimen #9 (hereinafter referred to as Specimen #2), which the author will model by following the methods of analyses as outlined in TEC 2007 and ASCE/SEI-41-06. Lap splice modelling recommendations as per the two documents will be compared to their respective experimental results.

Each physical test frame constructed in the laboratory is essentially a ½ scale 3-storey and 3-bay frame of the project's prototype reinforced concrete frame, but differs slightly with respect to code conformations and deficiencies. This ½ scaling is based on principles of equal stresses between the full scale prototype frame and the scaled test specimen, leading to half the displacements of the prototype frame but equal inter-storey drifts. The frames were subjected to simulated seismic excitation through the pseudo-dynamic testing procedure.

The following objectives are set forth in this thesis:

- Evaluation of pseudo-dynamic test results of two deficient reinforced-concrete frame specimens, one with lap splice deficiencies and one without;
- Calibration of OpenSees models of test specimens through numerical simulations and comparison of accuracies obtained from different modelling techniques;
- Investigation of local deformation components, and their interactions and contributions to the global response of the specimens using calibrated models;
- Present and comment on the effects of the presence of lap splices on local and global behaviours in the physical frame and computer models;
- Evaluation of strain-based nonlinear performance assessment procedures as outlined in TEC 2007 and the rotation-based nonlinear performance assessment procedures outlined in ASCE/SEI 41-06 in light of experimental observations; and
- Suggest future directions for an improved performance-based design and assessment code

Chapter 2 briefly presents an overview of the experimental setup and the specimens' results.

Numerical simulations of Specimen #1 and Specimen #2 are presented in Chapter 3 in comparison with experimental results and observations. Since Specimen #1 is the reference specimen without splices, the calibration of the computer model is also presented in Chapter 3. Special attention is given to the effects of lap splices in the deficient specimen. The modelling results of the various building code recommendations on accounting for deficient lap splices are compared with the experimental results. While the global behaviour of the results is examined, selected beams and columns are examined in detail on a local scale using the calibrated computer models of the test specimens. This

chapter also presents the results of the performance evaluations conducted on the specimens, along with comparisons to the experimental damages.

Lastly, in Chapter 4, a summary with the main conclusions of this thesis are presented with future research recommendations.

2. PSEUDO-DYNAMIC TESTING

2.1 General

Two specimens were built and tested at METU's Structural Mechanics Laboratory as a part of 108G034 Tübitak's project on performance-based design and assessment of reinforced-concrete buildings. Significant contributions in the laboratory were provided by Mehmet Engin Ayatar, Pourang Ezzatfar, and Mahdi Ghaffarinia. This chapter discusses the testing procedures and summarizes the experimental results for these two specimens.

Both specimens were deficient bare frames, as they were not compliant according to the provisions of TEC 2007. Deficiencies included the use of low strength concrete, plain reinforcing steel, minimum flexure reinforcement, insufficient confinement, and insufficient shear strength. Specimen #2 (referred to as SP2 in tables and figures) was essentially the same as Specimen #1 (referred to as SP1 in tables and figures), but with the presence of insufficient lap splices for column longitudinal reinforcement at plastic hinge regions (75% of the length required by TEC = 75% x $40d_b$). Specimen #1 had continuous bars throughout the beams and columns and Specimen #2 only had continuous bars throughout the beams.

The prototype structure's plan view is presented in Figure 2.1. The test frame of interest is the frame along gridline 3. As mentioned before, each test frame constructed in the laboratory was a ½ scale 3-storey and 3-bay frame of the project's prototype reinforced concrete frame. All frames were designed for a typical Turkish building located in the first seismic zone on Z3 (highly weathered soft metamorphic rock, medium dense sand and gravel, stiff clay and silty clay) soil type, with aforementioned deficiencies.

Continuous pseudo-dynamic testing was conducted for both specimens using synthetic ground motions compatible with the site-specific earthquake spectra developed for the city of Düzce, as a result of the earthquake which occurred in 1999.

Analytical verification of scaling of the test specimen and ground motions was verified by preliminary pushover and time-history analyses in the 1st project progress report (2010). When compressed in the time domain with a factor of $\sqrt{1/2}$ according to the similitude law, the original ground motion produced the desired earthquake demands on the ½-scaled prototype specimens.

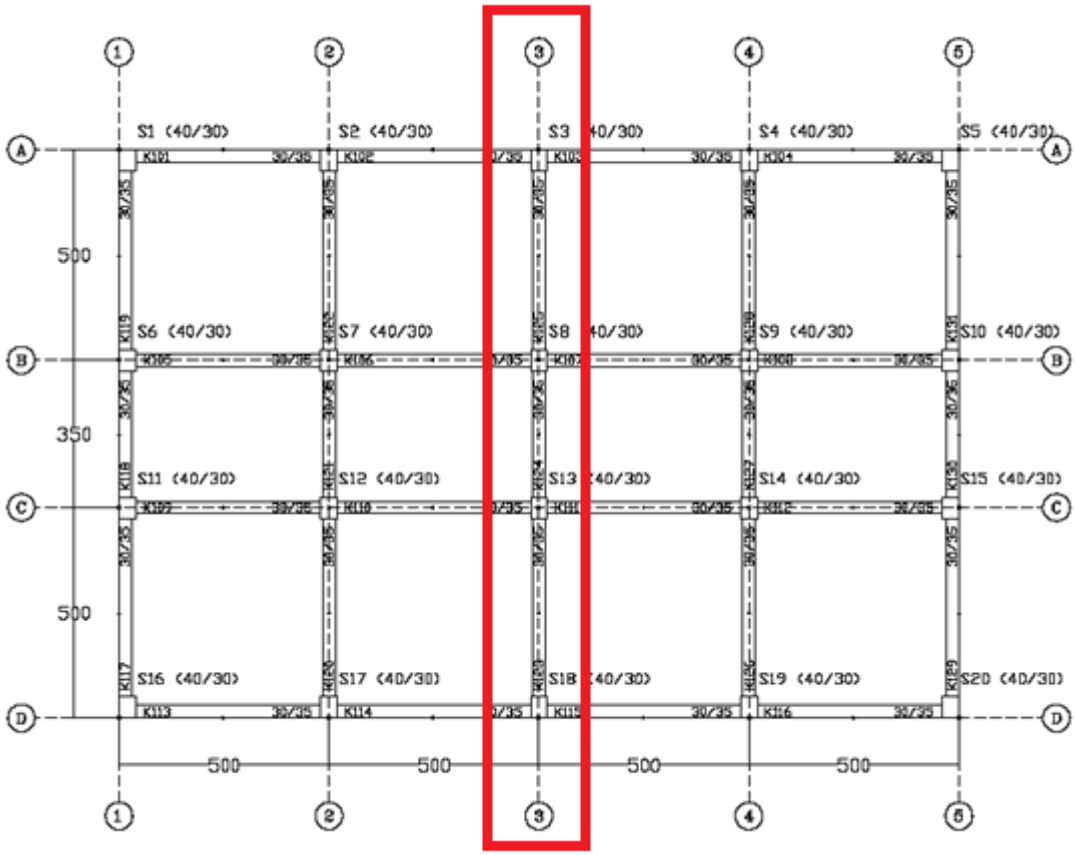

Figure 2. 1 Plan view of prototype building and test frame

2.2 Test Specimens

The member sizes and longitudinal reinforcement details of the prototype building was designed according to TEC 2007. The column dimensions were 400 mm x 300 mm with approximately a 1.33% longitudinal reinforcement ratio. The beam dimensions were 300 mm x 350 mm, which were uniform in all spans. The interior bay frame (Figure 2.1, gridline 3) was selected as the test specimen. The test specimens' dimensions were taken as ½ of the prototype frame member sizes, as shown in Figure 2.2, along with the notation for the beams and columns.

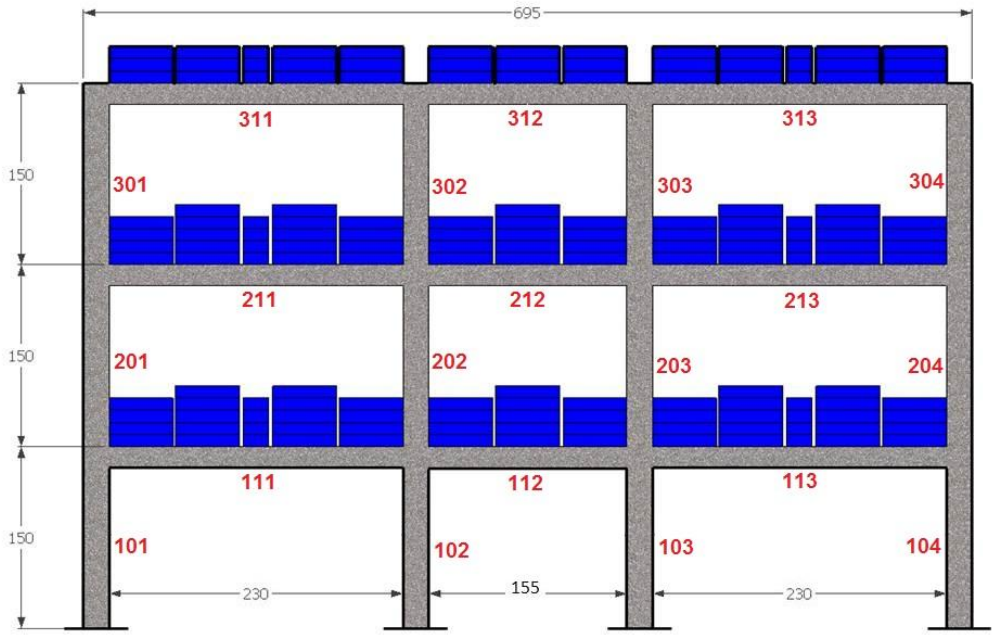

Figure 2. 2 Elevation view of the test specimens

The average uniaxial compressive strength of concrete used for Specimen #1 was 11.9 MPa. The column longitudinal reinforcement steel had a yield strength of 320 MPa, whereas the beam longitudinal reinforcement steel had 355 MPa, and the transverse reinforcement had 240 MPa, as determined from material tests. Detailed section drawings of Specimen #1, shown in Figure 2.3, were the same for the elements in each storey and each axis of the test frame.

The average uniaxial compressive strength of concrete used for Specimen #2 was 14.0 MPa. The reinforcement material strengths were the same as specimen #1, as the steel was obtained from the same batch. Specimen #2 had the same member dimensions as Specimen #1 and the only difference was that there was twice the amount of longitudinal reinforcing steel in the spliced regions.

In TEC 2007, the shear force demand on a column ($V_e = (M_t+M_b)/l_n$) is determined by using the top and bottom plastic moment values (M_t and M_b) of the columns, for a weak column-strong beam system, where l_n is the clear height. A weak column-strong beam system is defined in TEC 2007 when the plastic moments of the columns are less than 1.2 times the plastic moments of the beams connecting into a joint, which is the case for both specimens (see M_p values in Table 2.1 and Table 2.2). Most joints in the specimens satisfy this condition for a weak column-strong beam, with the exception being the exterior joints at the 1st and 2nd storeys.

The shear force resistance V_r is defined as:

$$V_r = 0.65 f_{ctd} b_w d + \frac{A_{sw}}{s} f_{ywd} d \tag{2.1}$$

where f_{ctd} is the concrete tensile strength, b_w is the column width, d is the column depth, A_{sw} is the area of the shear reinforcing steel, s is the spacing of the transverse reinforcing steel, and f_{ywd} is the strength of the transverse reinforcing steel.

The condition of insufficient shear capacity ($V_r < V_e$) corresponds to a shear-flexure failure mode (condition (ii) as defined by ASCE/SEI 41-06). In TEC 2007, there is no intermediate failure mode between shear and flexure failure defined and as such, this condition is classified as a shear failure mode.

Both specimens had deficient material strengths, reinforcement amounts, reinforcement details, and joint details. These deficiencies reflect the typical characteristics of the most common existing deficiencies in Turkey.

The properties of the test frames can be summarized as follows:

- The column longitudinal reinforcement was approximately 1.33%;
- Plain reinforcement bars with 8 mm and 10 mm diameters were used for the columns and beams, respectively;
- The yield strength of the 8 mm and 10 mm diameter bars were 320 MPa and 355 MPa, respectively;
- The ultimate strengths of these bars were 460 MPa and 555 MPa, respectively;
- 6 mm plain reinforcement bars were used as transverse reinforcement;
- The mean values of uniaxial concrete compressive strength (Specimen #1 – 11.9 MPa, Specimen #2 – 14.0 MPa) were determined from standard cylinder tests;
- The flexural and shear capacity of the beams were designed to be sufficient for gravity loads;
- The conventional strong-column weak-beam requirement was violated in these specimens;
- The transverse reinforcement spacing of the columns was kept constant throughout the column height, which resulted in unconfined zones at element potential plastic hinge regions; and
- Lateral reinforcements were absent at joints to reflect joint shear deficiencies

Detailed section and joint drawings of Specimen #1 and #2 are presented in Figure 2.3. The detailing was the same for the elements in each storey and each axis of the test frame.

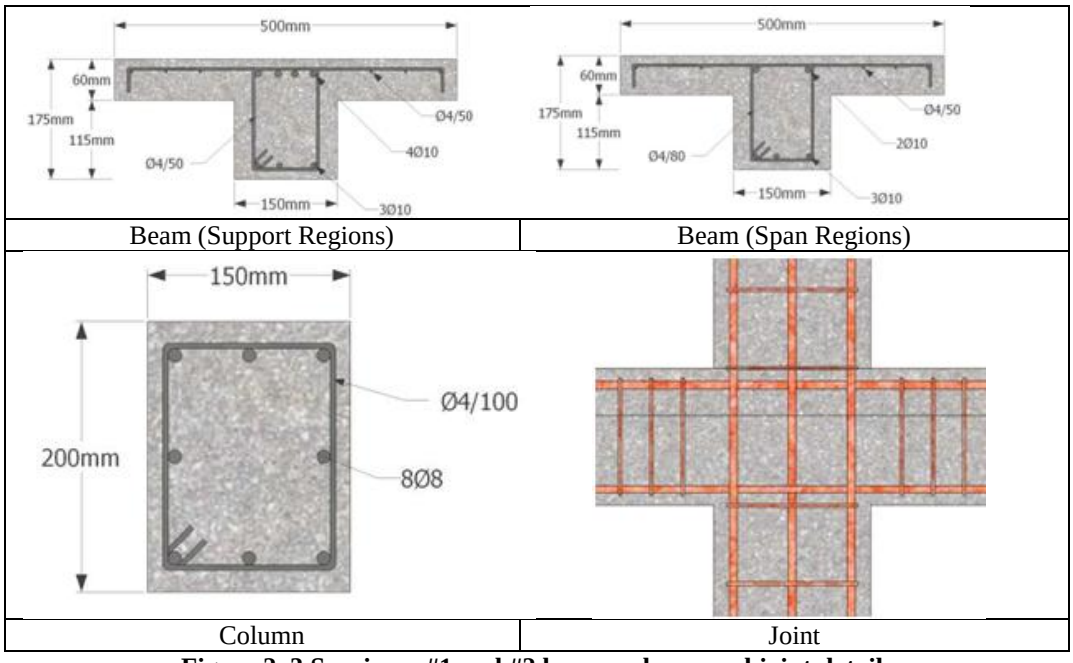

Beam (Support Regions)	Beam (Span Regions)
Column	Joint

Figure 2. 3 Specimen #1 and #2 beam, column and joint details

Longitudinal and shear reinforcement details, and moment capacities of columns and beams, calculated using the nominal strength values of both specimens, are presented in Table 2.1 and Table 2.2, respectively. For Specimen #2, moment capacities of column bases were calculated by applying the linear reduction suggested in TEC 2007 to the moment capacities of Specimen #1. Using ASCE/SEI 41-06's exponential reduction would have resulted in a higher resisting moment capacity and higher plastic moment capacity and thus, more conservative results. The top regions of columns in Specimen #2 had the same capacities as Specimen #1.

Table 2.3 presents the shear capacities and capacity/demand ratios of the columns, calculated using the nominal strength values (without safety factors) for the two frames according to TS 500 (2000). The columns in both specimens are not shear critical, as the ratios are greater than 1.0.

It should be noted again that all the reinforcement bars used in columns and beams of the both specimens were plain bars.

Table 2. 1 Reinforcement details and moment capacities of columns

Specimen	Reinforcement Details				Moment Capacity [kNm]	
	Long. (Mid)	Long. (End)	Lat. (Mid)	Lat. (End)	M_r	M_p
#1 (Outer)	8Ø8	8Ø8	2xØ4/100	2xØ4/100	11.4	13.6
#1 (Inner)					12.8	14.5
#2 (Outer)	8Ø8	16Ø8	2xØ4/100	2xØ4/100	8.6	10.2
#2 (Inner)					9.6	10.9

Table 2. 2 Reinforcement details and moment capacities of beams

SP	Reinforcement Details				Moment Capacity [kNm]			
	Long. (Support, i)	Long. (Span, ii)	Trans. (Support, i)	Trans. (Span, ii)	M_r(i)	M_r(ii)	M_p(i)	M_p(ii)
#1	4Ø10+3Ø10	2Ø10+3Ø10	Ø4/50	Ø4/80	17.9	11.9	20.7	16.3
#2	4Ø10+3Ø10	2Ø10+3Ø10	Ø4/50	Ø4/80	18.1	12.1	20.9	16.9

Table 2. 3 Column shear capacities, demands, and capacity/demand ratios

Specimen	V_r [kN]	V_e [kN]	V_r/V_e
#1 (Outer)	26.6	19.8	1.34
#1 (Inner)	26.6	21.1	1.26
#2 (Outer)	29.0	17.3	1.68
#2 (Inner)	29.0	18.5	1.57

2.3 Testing and Instrumentation

The dead and live loads remained constant throughout each pseudo-dynamic test. Gravity dead loads were applied through the use of steel blocks, as shown in Figure 2.2. The blocks were arranged such that the ratio of axial load to the axial load carrying capacity of the columns of the specimens is similar to the prototype frame. The axial load ratios of columns under gravity loads are presented in Table 2.4, where N is axial load experienced at the columns from the self-weight of the frame and the steel blocks which account for the transverse beams and slabs, and $N_o = f'_c A_c$ is the axial load carrying capacity of the columns.

Table 2. 4 Concrete strength and axial load ratios of columns

SP	Mean f'_c [MPa]	1st Storey N/N_o Ratio	
		Inner Columns	Outer Columns
#1	11.9	0.228	0.133
#2	14.0	0.195	0.114

Pseudo-dynamic testing is a hybrid earthquake simulation technique which combines numerical modelling of the structural properties with a physical test run in parallel with computations (Takanashi et al. (1975), Mahin and Shing (1985), Nakashima (1985)). This testing method was developed as an alternative to shake table testing. Through pseudo-dynamic testing, it is possible to accurately simulate large-scale structural behaviour under seismic loads in a more practical way. Due to the "pseudo-time" nature of the method, the general behaviour of the structure under the earthquake loads can be closely monitored during the experiment.

In each pseudo time-step, restoring forces are measured by the load cells and the information collected is used with the pre-defined input ground motion, mass, and damping properties to determine the step-by-step numerical integration through the equation of motion. The displacements for the successive steps are calculated and applied to the lateral degrees of freedom of the test structure through servo-controlled hydraulic actuators. This is shown graphically in Figure 2.4 for the case of the test specimens, which have three degrees of freedom.

Figure 2. 4 Test specimen and pseudo-dynamic testing system scheme

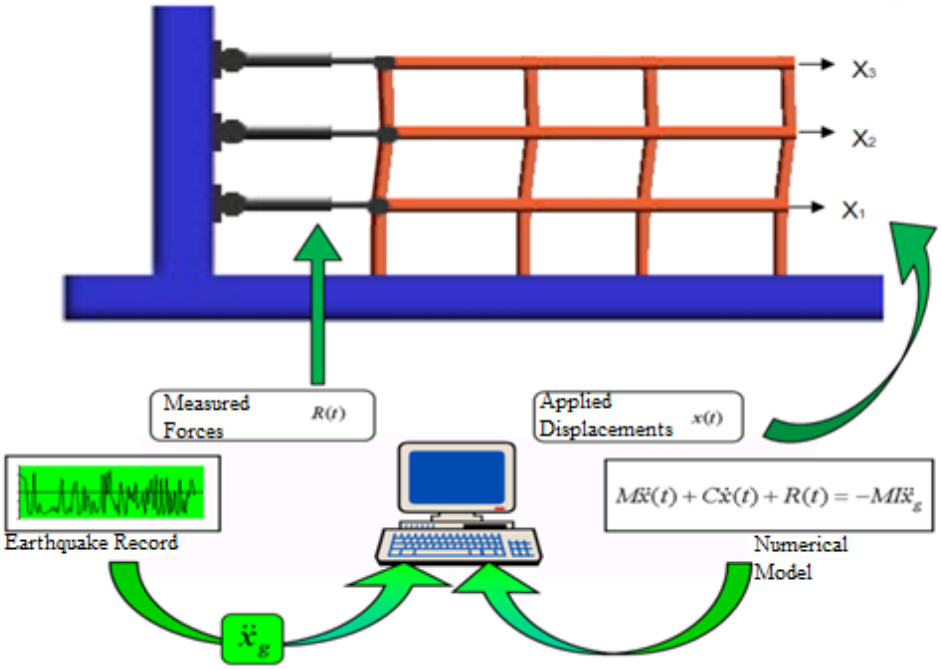

Figure 2.4 (Continued)

Ground motions used for the pseudo-dynamic tests were synthetic-time acceleration series of the 1999 Düzce earthquake, which were generated in a previous work package of the Tübitak research project. They were compatible with the site-specific earthquake design spectra for different probabilities of exceedance on different soil types, as shown in Table 2.5. Three of the generated acceleration series from the previous work package (named D1, D2, and D3) were imposed on the test specimens subsequently. Acceleration time series with the order of application and corresponding spectra of the ground motions are shown in Figure 2.5.

Table 2. 5 Ground motion properties

Earthquake GM	Probability of Exceedance (50 Years)	Soil Class/Type	PGA [g]
D1	50%	Z1/Rock	0.254
D2	10%	Z1/Rock	0.545
D3	10%	Z3/Soft Soil	0.604

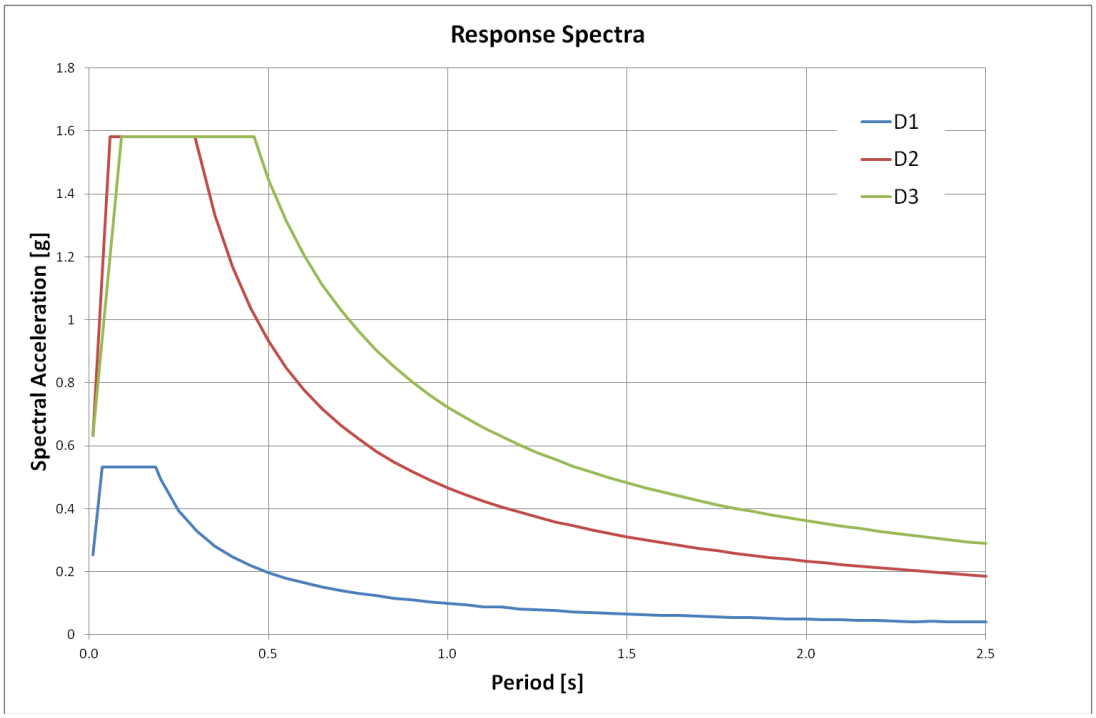

a) Design Response Spectra

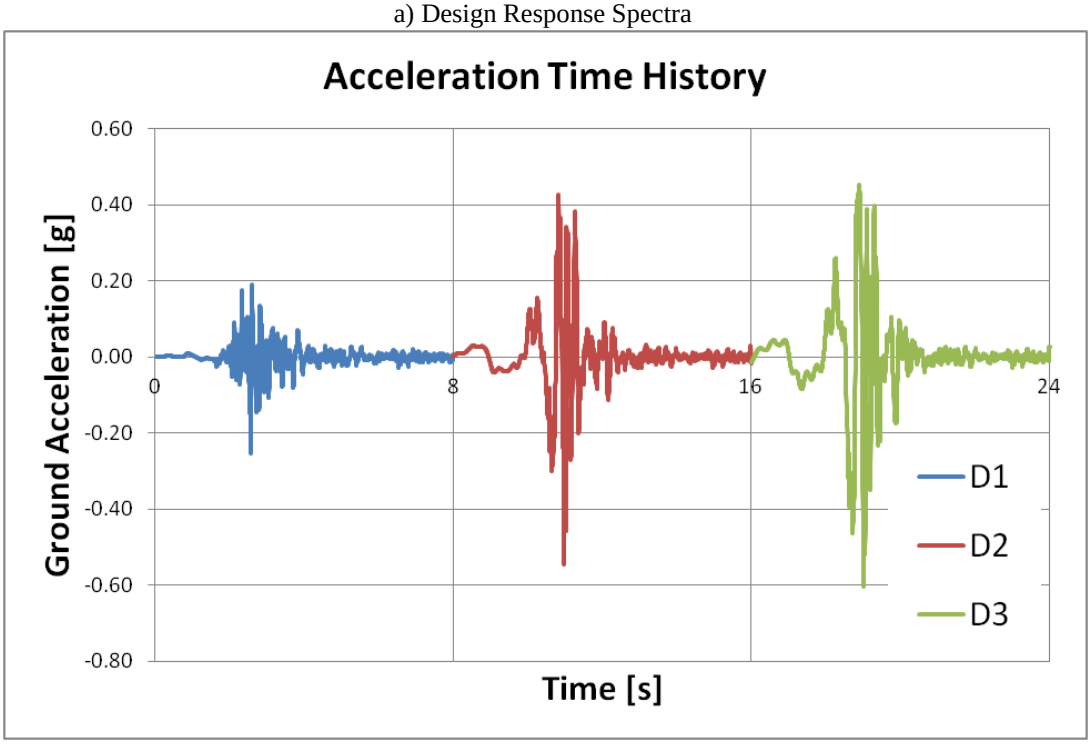

b) Acceleration Time History

Figure 2. 5 Response and acceleration spectra

Forces applied on the specimen were measured by the load cells built in the actuators of the pseudo-dynamic testing system at each storey of the test frames. Linear Variable Differential Transformers (LVDTs) were used to measure the storey displacements and the displacements at the column and

beam ends of the 1st and 2nd storeys. Transducer boxes at the 1st storey outer columns were used to measure the axial loads, shear forces, and moments. The configuration is shown in Figure 2.6.

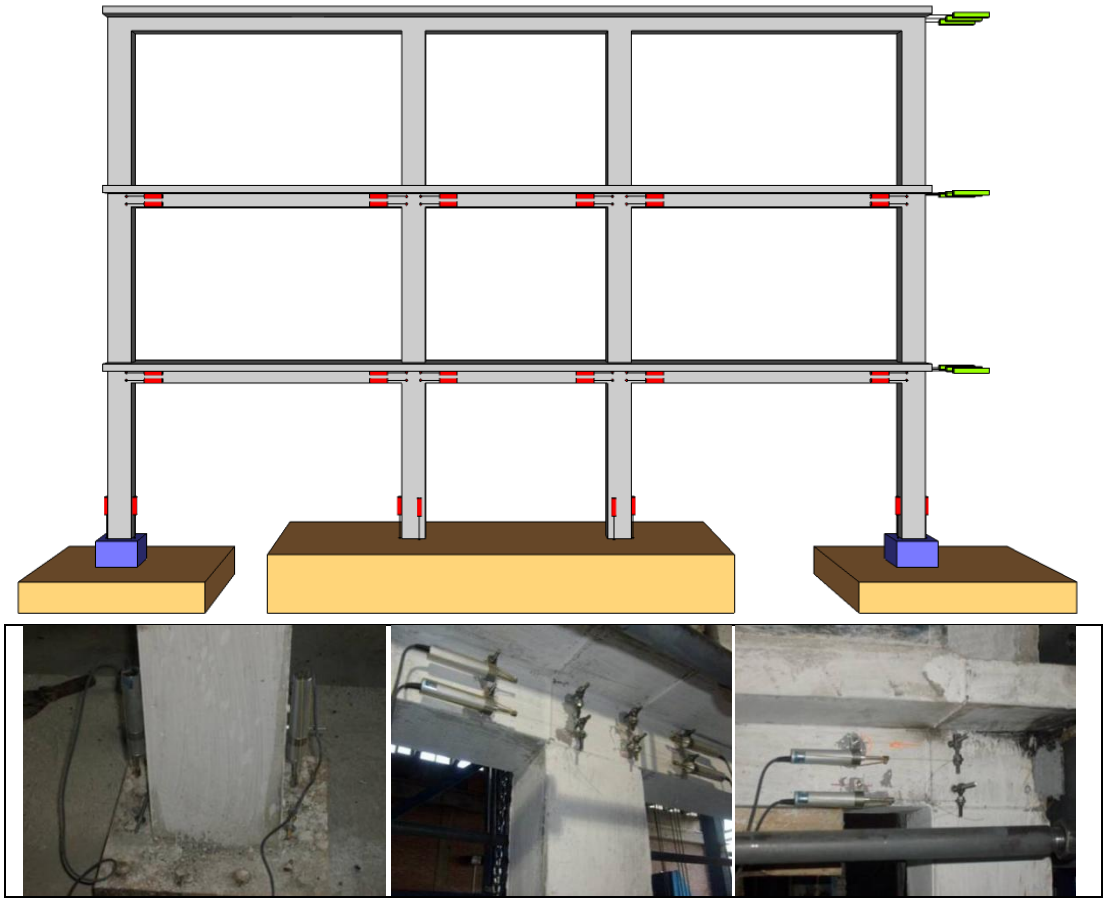

Figure 2. 6 Measurement devices and their configurations

2.4 Test Results

Test results of both specimens are presented in this section. Storey displacements, inter-storey drift ratios, and storey shear forces are presented, along with selected pictures showing certain damages observed. Local demand parameters such as member end curvatures are discussed in the next chapter, along with the numerical simulation results.

2.4.1 Specimen #1

The roof displacement time history response from the physical test is presented in Figure 2.7 along with the damages observed at selected peak deformations. The inter-storey drift ratio time history responses are presented in Figure 2.8. No damage was observed under D1, and the inter-storey drift ratio was under 0.3% for each storey and the maximum roof displacement was 9.4 mm. The specimen was in a minimum damage state after D1.

Under D2, the maximum inter-storey drift ratio experienced was 1.3% and the maximum roof displacement was 49 mm. Major damages observed during D2 were flexural cracks in both the interior and exterior columns of the 1st storey, and the onset of visible cracks in the 1st storey joint regions (which initiated prior to cracks in the connecting beam and column ends). Both of these

damage formations were directly related to the lack of confinement in column ends and joint regions. This implies that some inelastic deformations occurred in the 1st storey and parts of the specimen were at most in a moderate damage state after D2.

Under D3, the macro-cracks at the bottom ends of the 1st storey columns continued to spread and widen. Damages in the columns were followed by the spread of inclined crack in the joint regions and flexural crack formations at the beam ends. The 1st storey drift ratio reached a maximum value of 4.1% and the maximum roof displacement reached a maximum value of 206 mm. The spread of damage in the upper stories was in the form of shear cracks in the joints and flexural cracks in the upper ends of the 2nd and 3rd storey columns. Inter-storey drift ratios of the higher storeys were higher than 5%, greater than the 1st storey. The large deformations during the ground motions resulted in high residual displacements towards the end of the pseudo-dynamic test. Large cracks at the top ends of the 3rd storey columns indicated that longitudinal reinforcement slip occurred. Figure 2.9 shows damages observed at the top of the 3rd storey columns, due to the lack of anchorage at that location. The structure was in a severe damage state after D3.

Shear force vs. inter-storey drift ratio for each storey and base shear vs. roof displacement plots are presented in Figure 2.10. The base shear vs. roof displacement plot shows severe strength degradation and a softening response, implying that the specimen lost its lateral load carrying capacity.

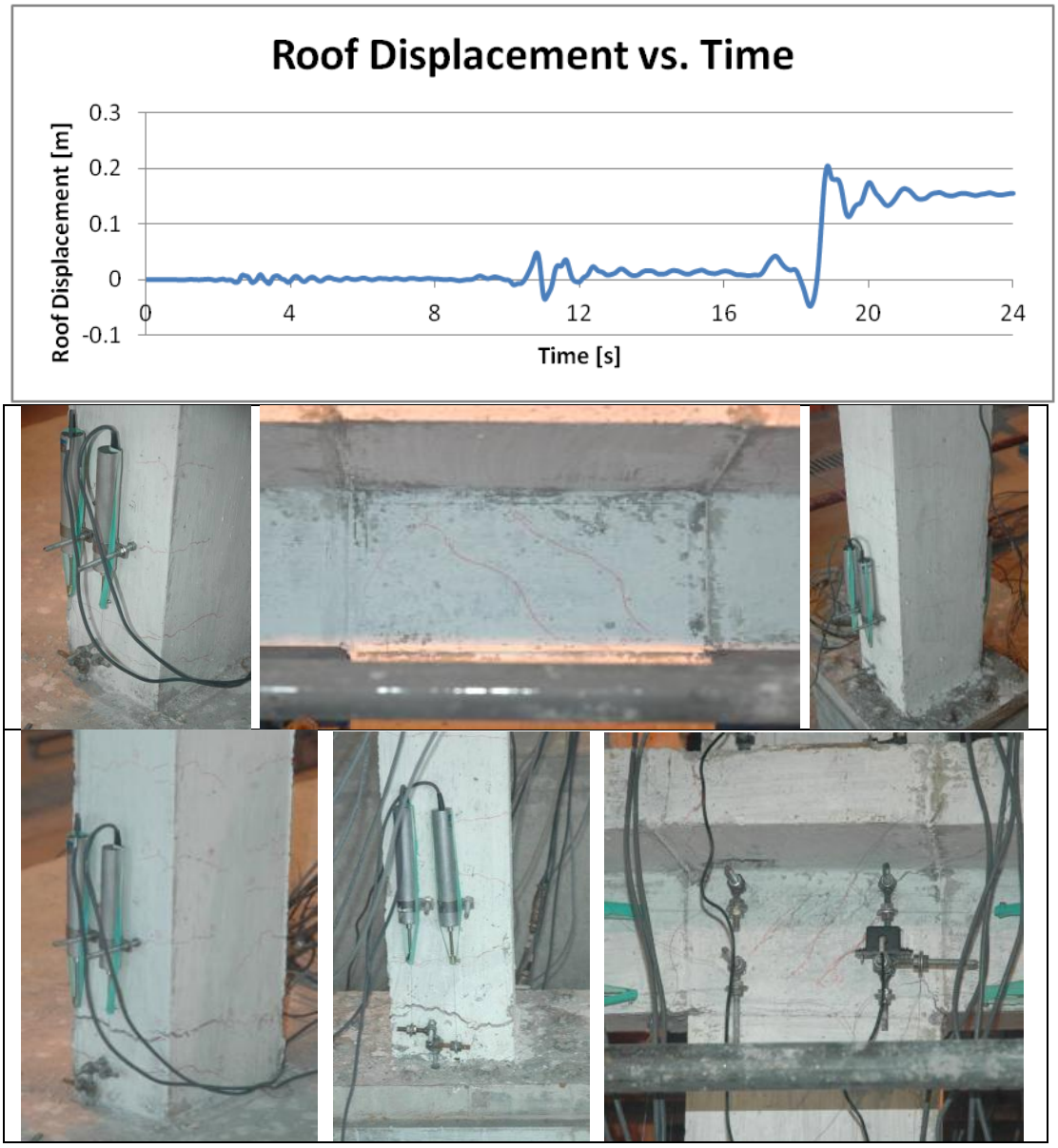

Figure 2. 7 Roof displacement time history/observed damages (SP1)

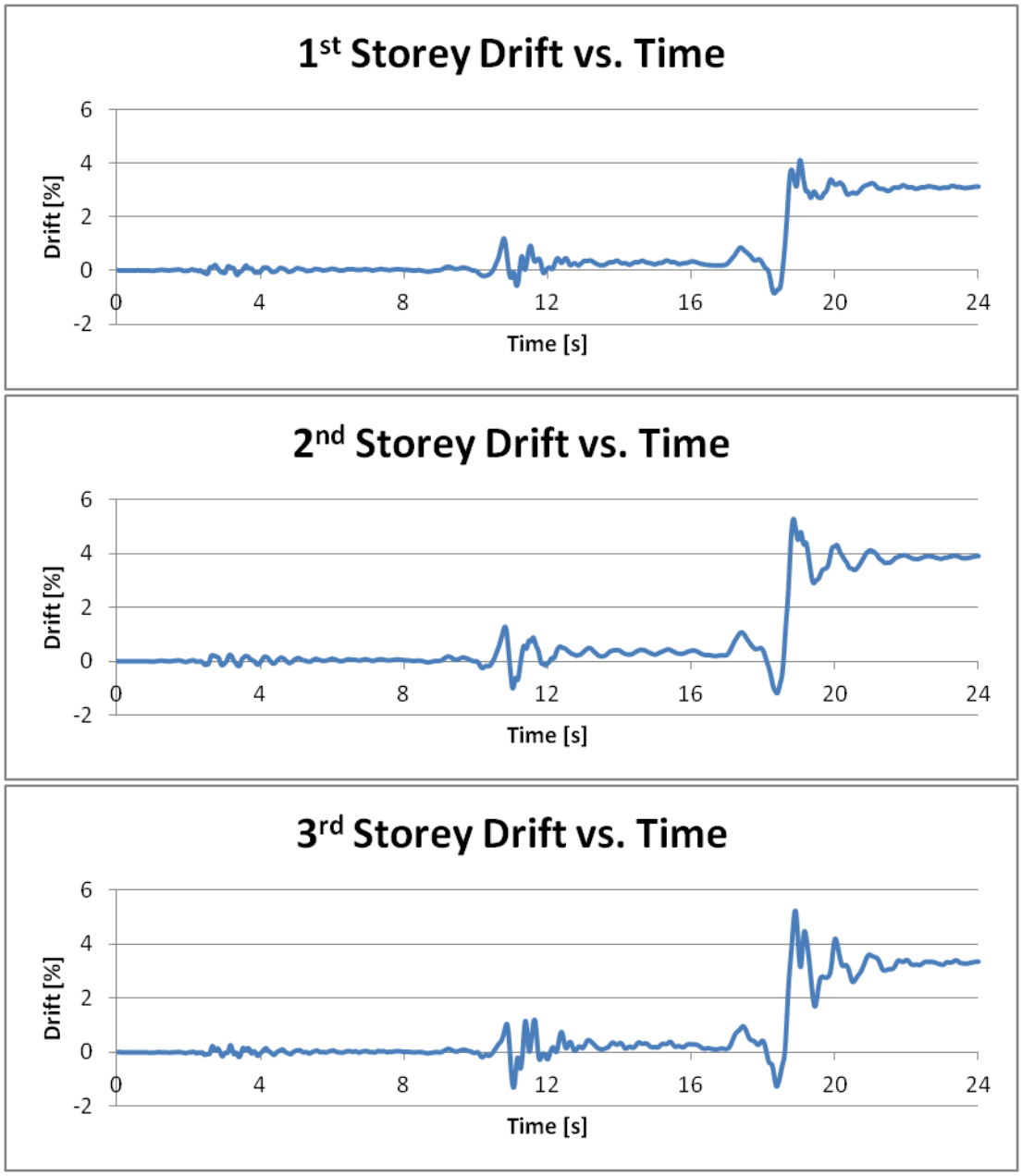

Figure 2. 8 Inter-storey drift ratio time histories (SP1)

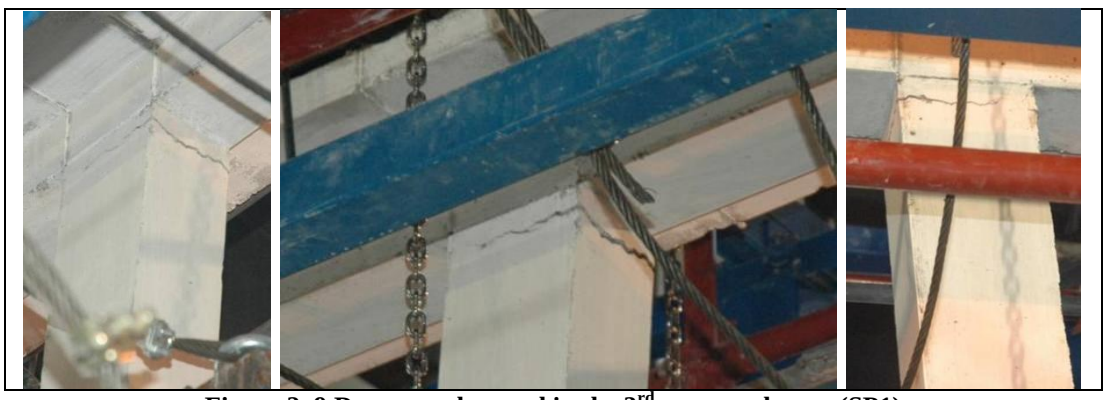

Figure 2. 9 Damages observed in the 3rd storey columns (SP1)

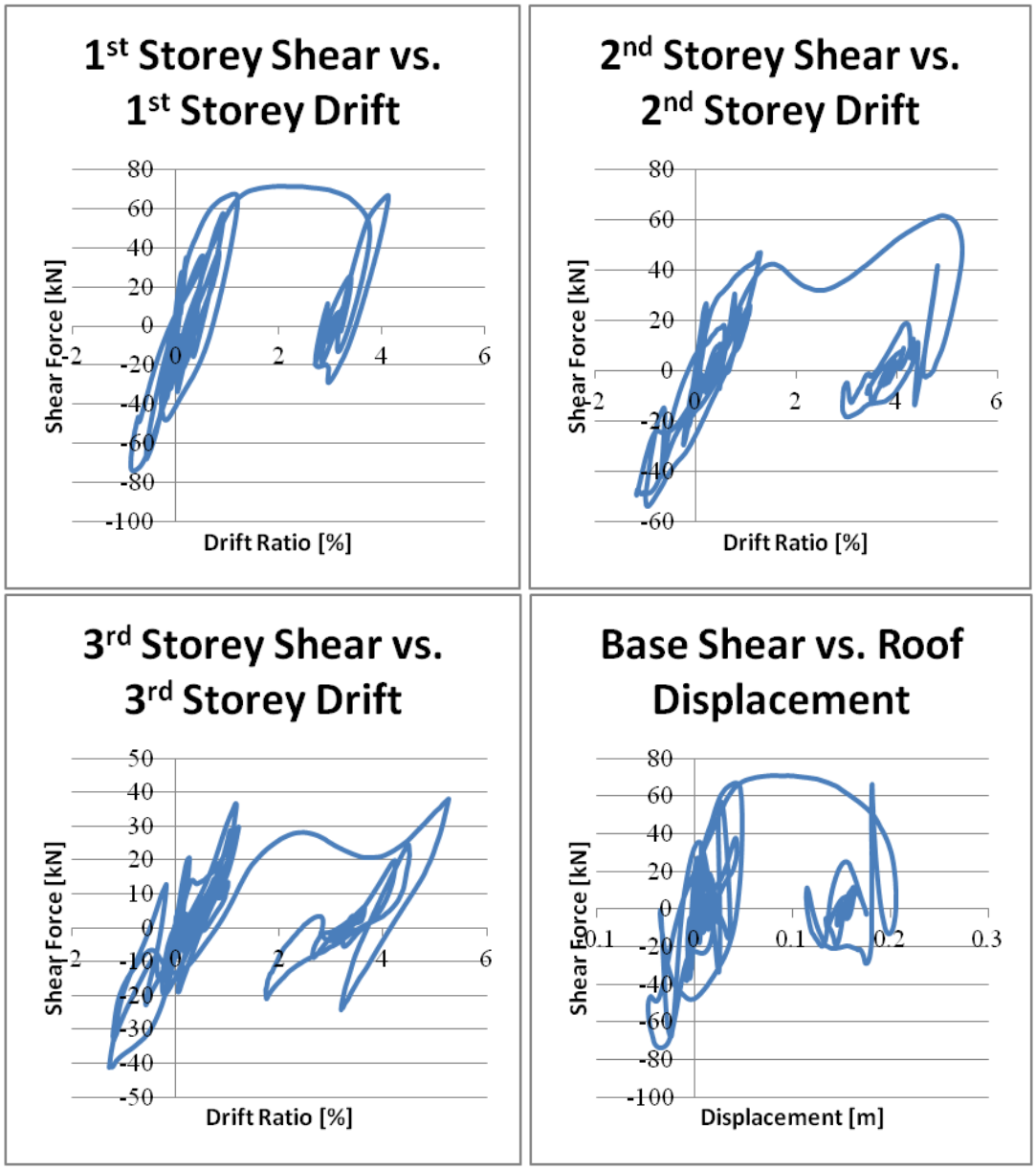

Figure 2. 10 Storey shear forces vs. drift response (SP1)

2.4.2 Specimen #2

The roof displacement time history response from the physical test is presented in Figure 2.11, along with the damages observed at selected peak deformations (Figure 2.12). The inter-storey drift ratio time history response is presented in Figure 2.13. No damage was observed under D1, and the inter-storey drift ratio was under 0.3% for each storey whereas the maximum roof displacement was 9.3mm. The specimen was in a minimum damage state after D1. Minor cracks were observed at the 1st storey columns at the peak of D1.

Under D2, the maximum inter-storey drift ratio experienced was 1.2% and the maximum roof displacement was 55.1mm, similar to the values of Specimen #1. Major damage observed during D2 was flexural cracks in both the interior and exterior columns of the 1st storey, and the onset of visible cracks in the 1st storey joint regions (which initiated prior to cracks in the connecting beam and column ends). Both of these damage formations were directly related to the lack of confinement at

column ends and joint regions. This implies that some inelastic deformations occurred in the 1st storey and the specimen was at most in a moderate damage state after D2, once again much like Specimen #1. However, there was very little residual displacement observed after D2, contrary to that observed in Specimen #1.

Under D3, the macro-cracks at the bottom ends of the base columns continued to spread and widen. Damages in the columns were followed by the spread of inclined cracks in the joint regions and flexural crack formations at the beam ends. The 1st storey drift ratio reached a maximum value of 4.3% and the maximum roof displacement reached a maximum value of 153 mm. Compared to Specimen #1, the 1st storey drift ratio was similar, but the maximum roof displacement is significantly reduced. The spread of damage in the upper stories was in the form of shear cracks in the joints and flexural cracks in the upper ends of the 2nd and 3rd storey columns. Maximum inter-storey drift ratios of the 2nd and 3rd storeys were 3.2% and 3.5%, respectively. The large deformations during the ground motions did not result in high residual displacements, as was observed in Specimen #1. This can be attributed to the presence of lap splices, which provided additional resisting forces in the spliced regions. Large cracks at the ends of the columns indicated that the longitudinal reinforcement pullout phenomenon due to the unconfined joints was also experienced, as shown in Figure 2.14. Contrary to Specimen #1, there was no yielding at the top of the 3rd storey columns. The structure was in a severe damage state after D3.

Shear force vs. inter-storey drift ratio for each storey and base shear vs. roof displacement plots are presented in Figure 2.15. The base shear vs. roof displacement plot does not show as severe strength degradation and softening response as Specimen #1, implying that the specimen had a comparatively larger lateral load carrying capacity after the ground motions.

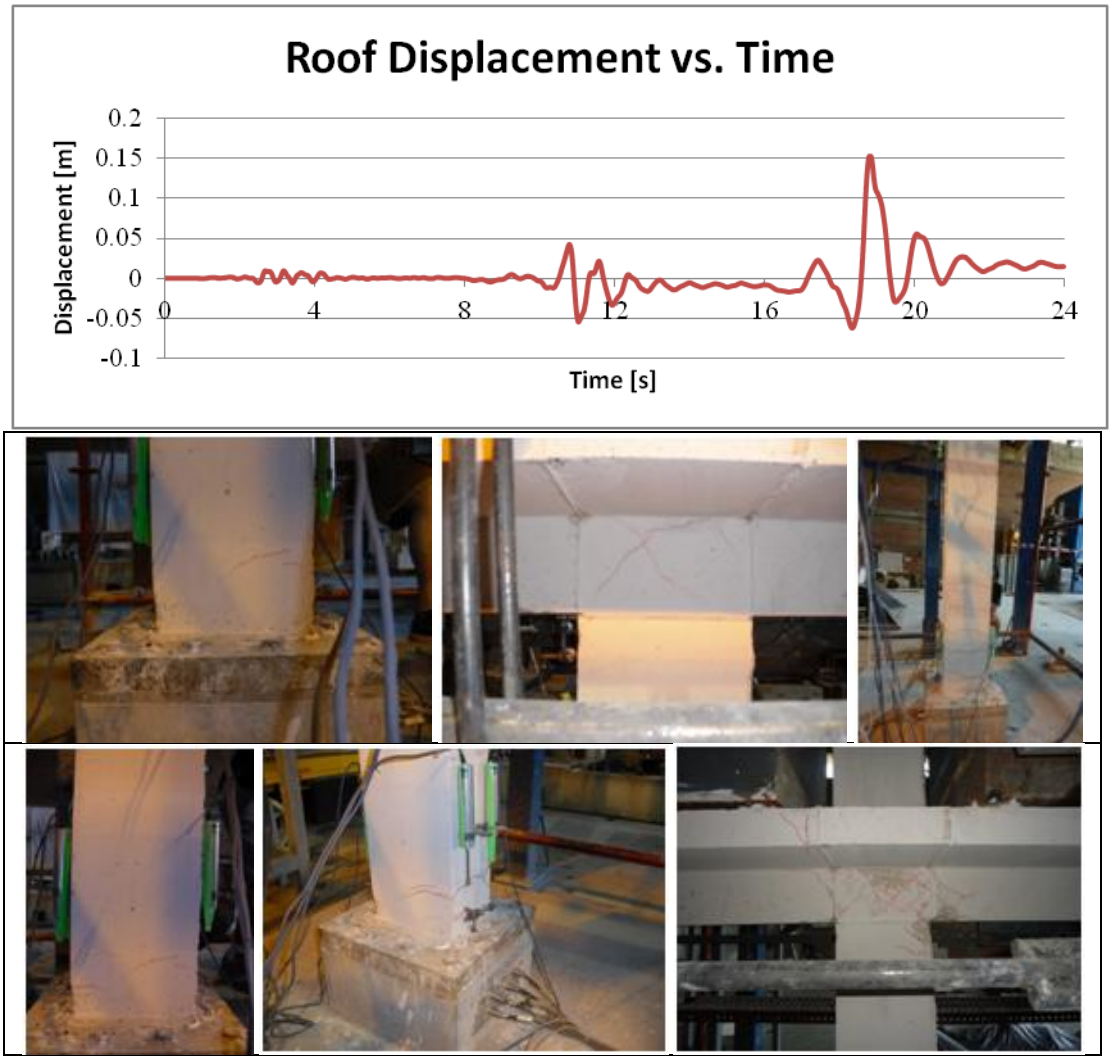

Figure 2. 11 Roof displacement time history/observed damages (SP2)

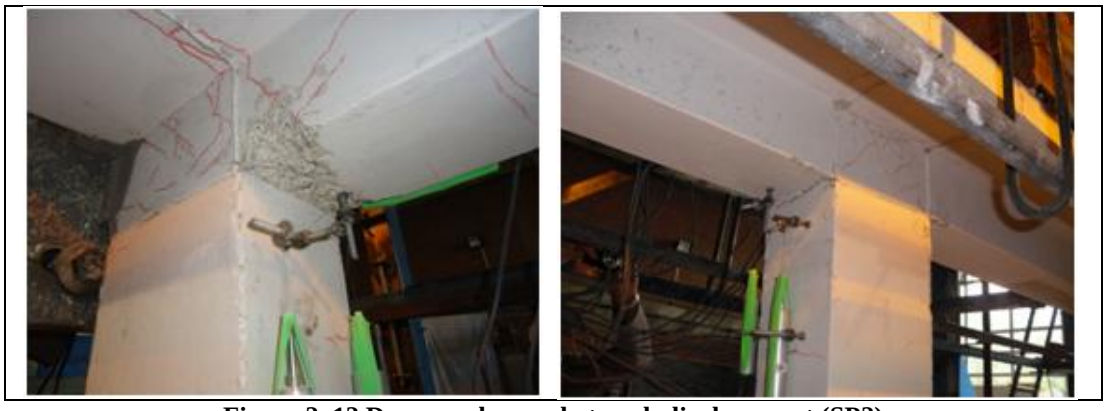

Figure 2. 12 Damage observed at peak displacement (SP2)

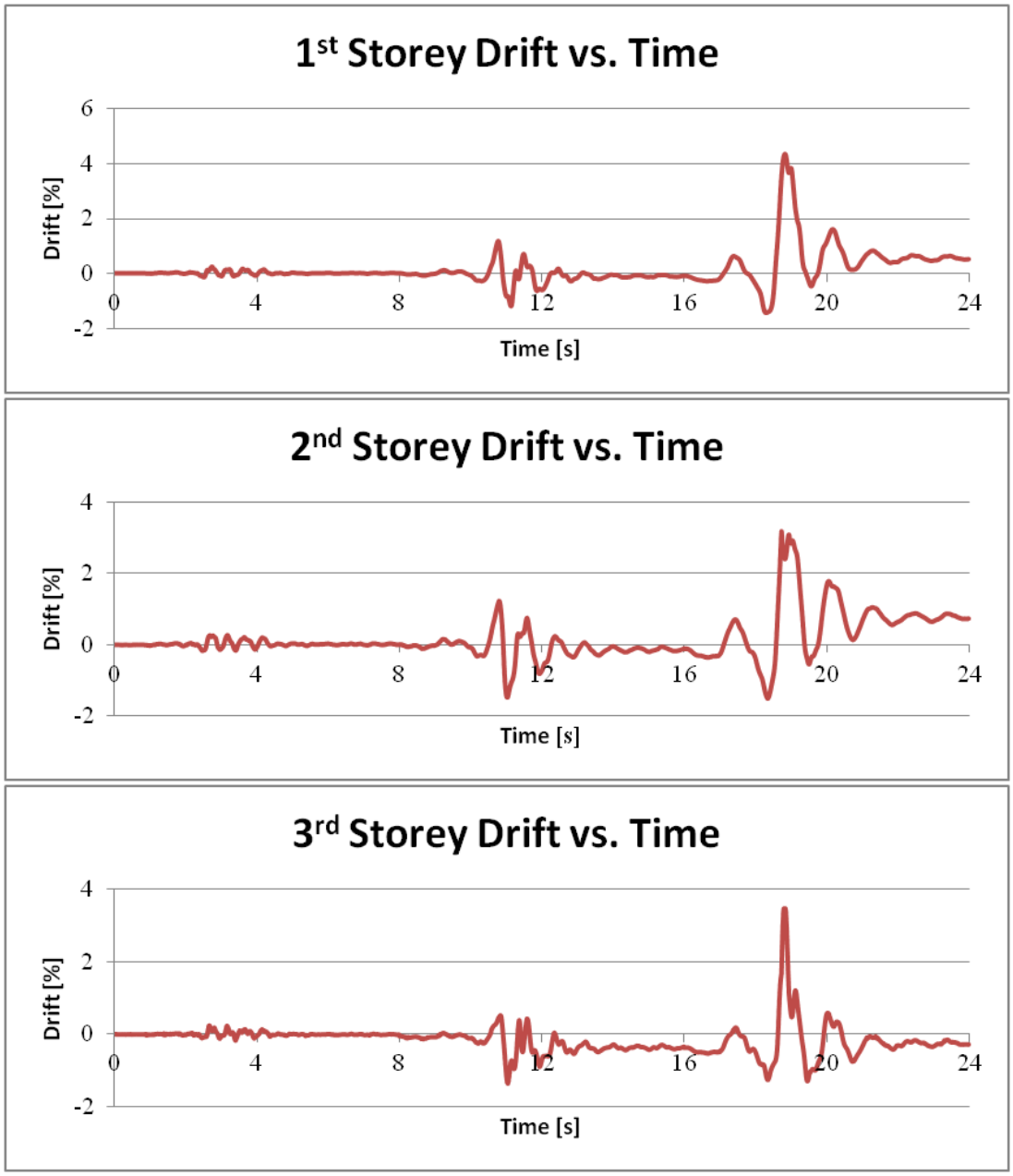

Figure 2. 13 Inter-storey drift ratio time histories (SP2)

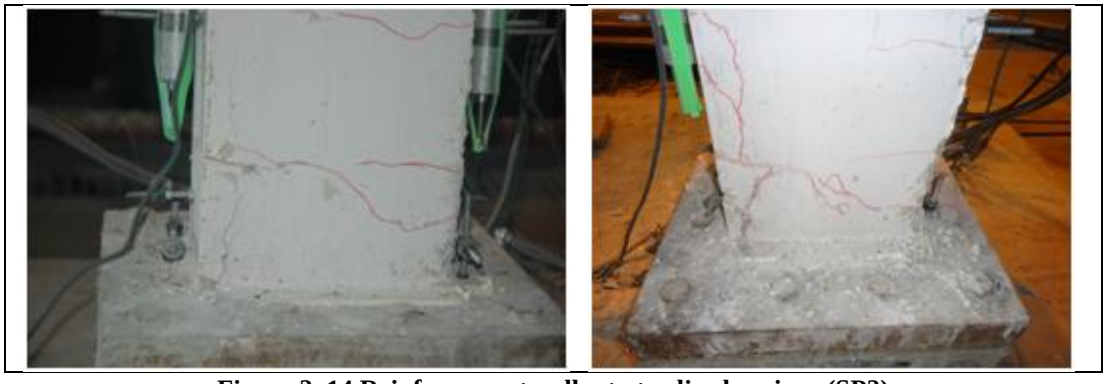

Figure 2. 14 Reinforcement pullout at spliced regions (SP2)

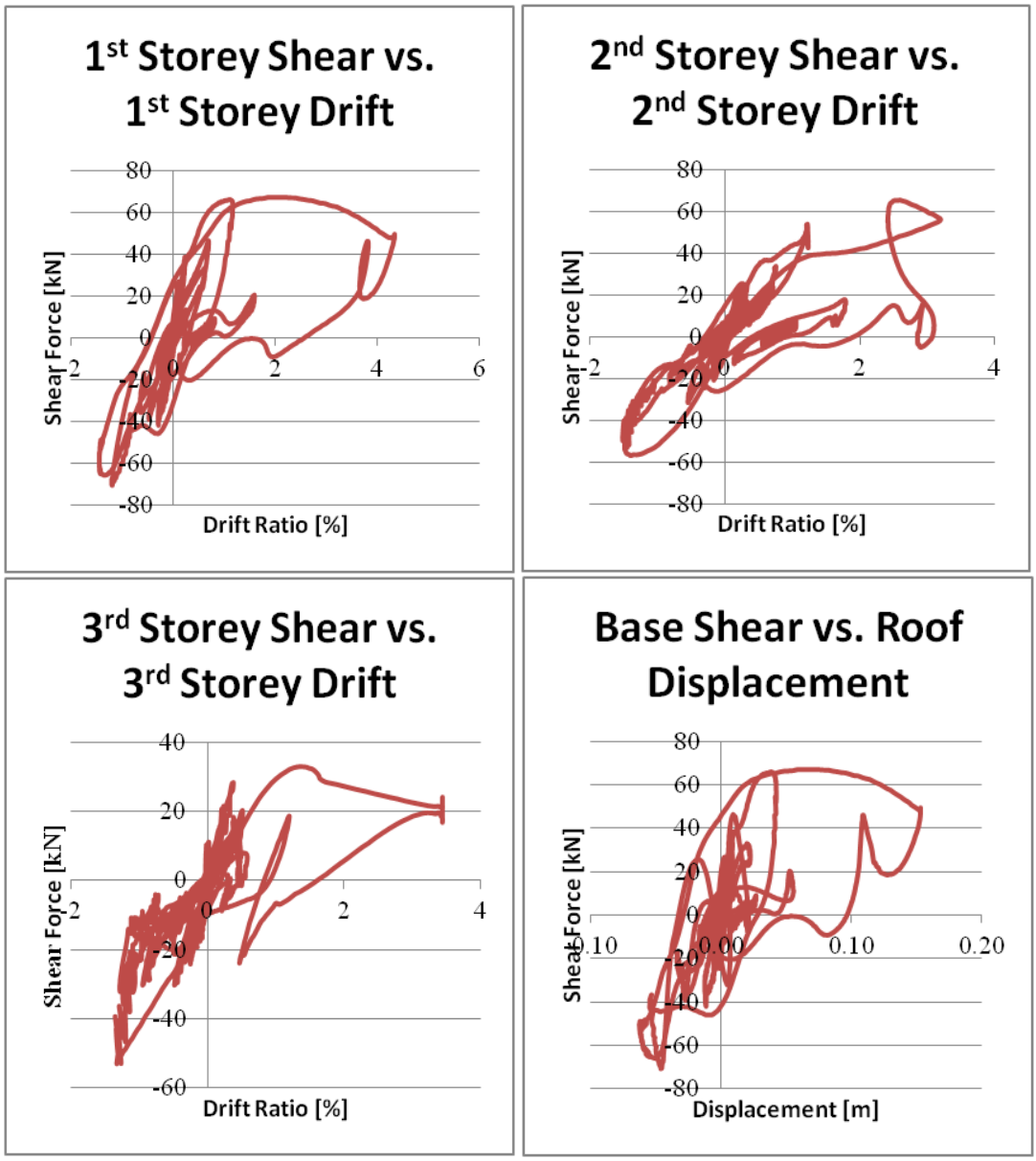

Figure 2. 15 Storey shear force vs. drift response (SP2)

2.5 Comparison of Test Results

Comparisons of the two specimens are presented in terms of the 1st storey drift ratio, base shear vs. roof displacement response, selected beam/column rotations, and vibration periods of the 1st mode.

It should be reminded that ideally, the only difference between the two deficient specimens is the presence of insufficient lap splices. However, other inherent factors to consider such as construction methods, material strengths, and power outages during the pseudo-dynamic tests affected the results of the experiments. Thus, these comparisons are presented in this section without detailed discussion as this may lead to misleading interpretations.

The 1st storey drift ratio time histories for both specimens are presented in Figure 2.16. Base shear vs. roof displacement responses are shown in Figure 2.17 and maximum recorded values of these responses are provided in Table 2.6. Figure 2.18 shows the 1st period vibration mode variation time

history plots. Figure 2.19 shows the rotation time histories for column 101's bottom end and beam 111's left end.

The fundamental periods were determined by the procedures defined by Molina et al. (1999), where the experimental displacements *u(n)*, velocities *v(n)*, and restoring forces' *r(n)* relation is:

$$\begin{bmatrix} u^T(n) & v^T(n) & 1 \end{bmatrix} \cdot \begin{bmatrix} K^T \\ C^T \\ o^T \end{bmatrix} = r^T(n) \tag{2.2}$$

where *K* and *C* are the secant stiffness and viscous equivalent damping matrices, respectively. *o* is a constant force offset term. The equation contains "$2 \cdot ndof^2 + ndof$" unknowns and the number of available equations is "$N \cdot ndof$", for *N* time intervals. By satisfying the condition that $N > 2 \cdot ndof + 1$ and estimating *K* and *C* by a least mean squares algorithm, the complex eigen-frequencies and mode shapes can be determined by solving the generalized eigenvalue equation:

$$s \begin{bmatrix} C & M \\ M & 0 \end{bmatrix} w + \begin{bmatrix} K & 0 \\ 0 & -M \end{bmatrix} w = 0 \tag{2.3}$$

where *M* is the theoretical mass matrix, *w* contains the eigenvectors, and *s* is the conjugate couples of eigenvalues.

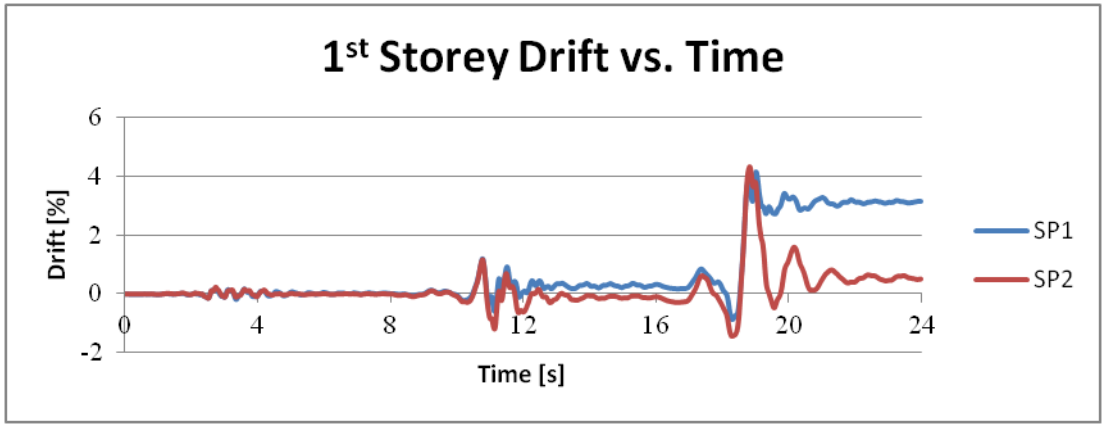

Figure 2. 16 1st Storey drift time history comparisons

It is observed that the drift response is similar for both specimens during D1 and D2. However, a major difference observed during D3 is the residual deformations present in Specimen #1. This can be attributed to the major structural deficiencies that result in significant strength degradation and less energy dissipation as shown in Figure 2.17. Specimen #2 did not have such an exaggerated residual displacement. In specimen #1, the sudden failure during D3 in the relatively weaker structure leads to a larger residual drift.

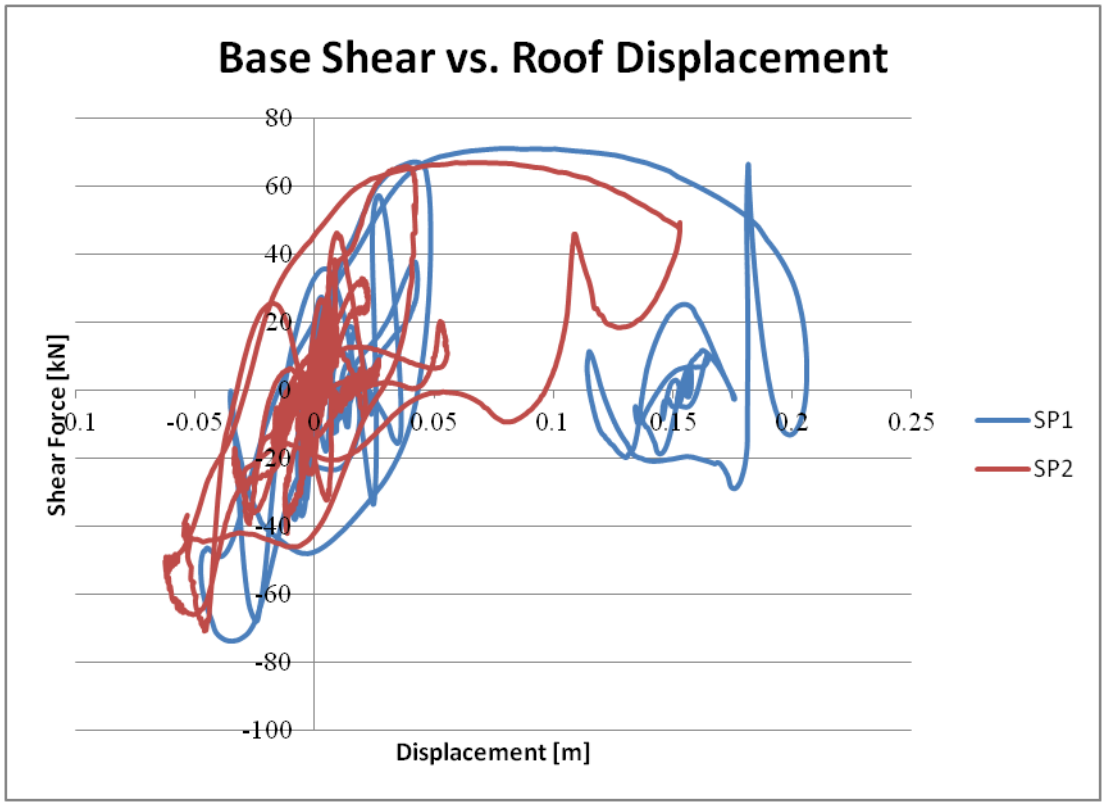

Figure 2. 17 Base shear vs. roof displacement comparison

Table 2. 6 Maximum base shear, roof displacement and 1st storey drift comparisons

Ground Motion	Max Base Shear [kN]		Max Roof Displacement [mm]		Max 1st Storey Drift [%]	
	SP1	SP2	SP1	SP2	SP1	SP2
D1	36.6	38.3	9.4	9.3	0.21	0.24
D2	68.5	71.0	48.7	55.1	1.21	1.19
D3	75.1	67.0	206.0	153.2	4.13	4.34

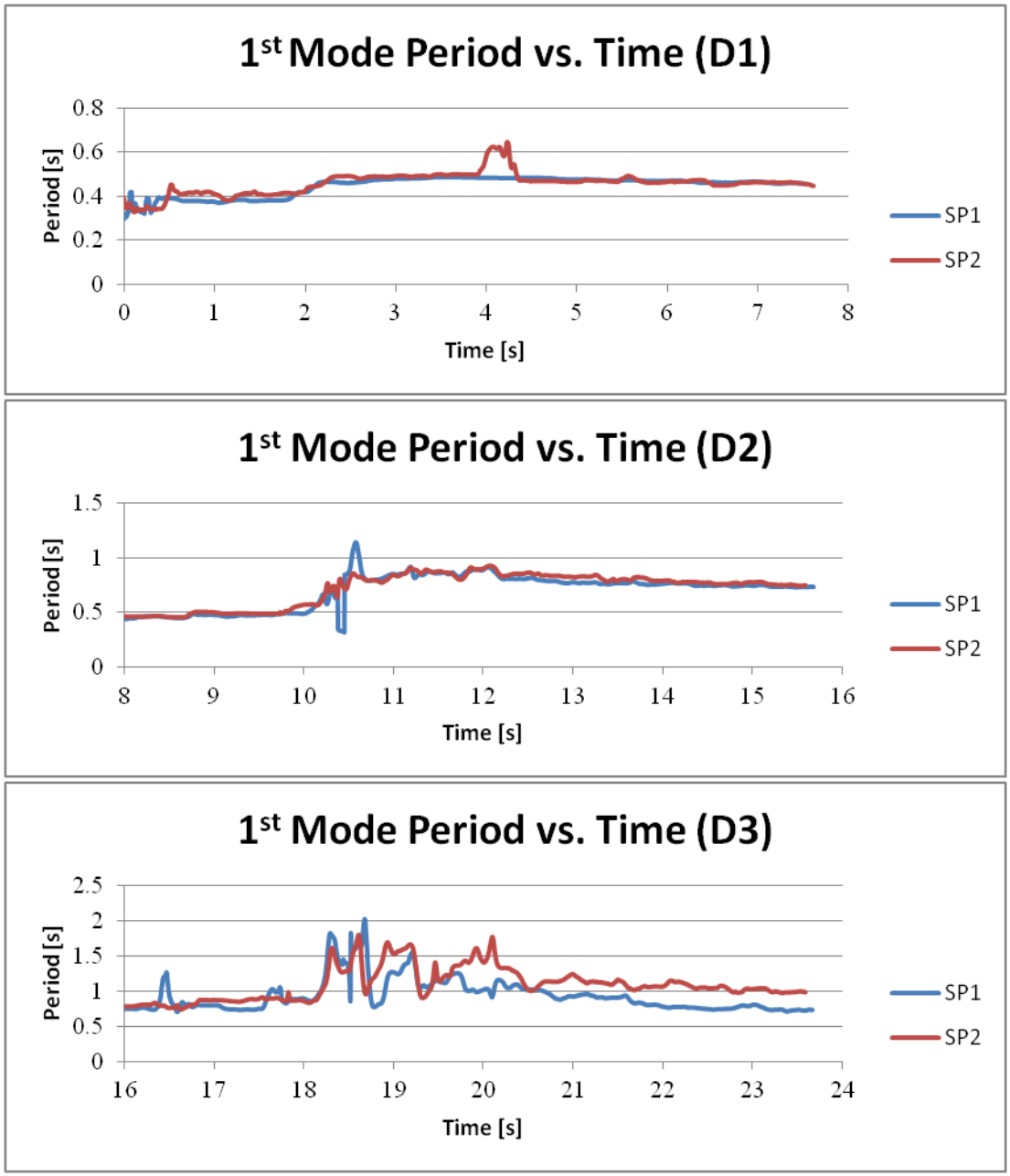

Figure 2. 18 1st mode period time history comparisons

The identified period for Specimen #1 increased from 0.35 seconds at the beginning of D1, to 0.5 seconds at the end of D1, due to cracking. The onset of visible plastic deformations occurred during D2 and resulted in a period of 0.8 seconds. The period vs. time plot exhibited some oscillations and spikes which correspond to large plastic behaviour between 10 seconds and 11 seconds. During D3, the period varied between 0.8 seconds and 1.0 seconds, with the exception of a few spikes between 18 seconds to 20 seconds, reaching a maximum of approximately 2.0 seconds during this range. These spikes were also affiliated with the extensive damages observed during this time.

In Specimen #2, the period also started at 0.35 seconds and increased to 0.5 seconds towards the end of D1. One visible difference between the two specimens during D1 is that there is a spike to a period

of 0.65 seconds for Specimen #2. One possible explanation is that there was a power outage during this time, leading to this artificial peak as there were no visible damages during this ground motion.

The pattern observed during D2 was similar to the behaviour of Specimen #1, but the period variation between 10 seconds and 11 seconds was not as extreme. The peaks of the earthquake did not affect Specimen #2 as much as Specimen #1.

The largest variations between the two specimens occurred during D3. Extensive damages were observed for both specimens during D3, but it seems that the peaks of the earthquake once again did not affect Specimen #2 as much.

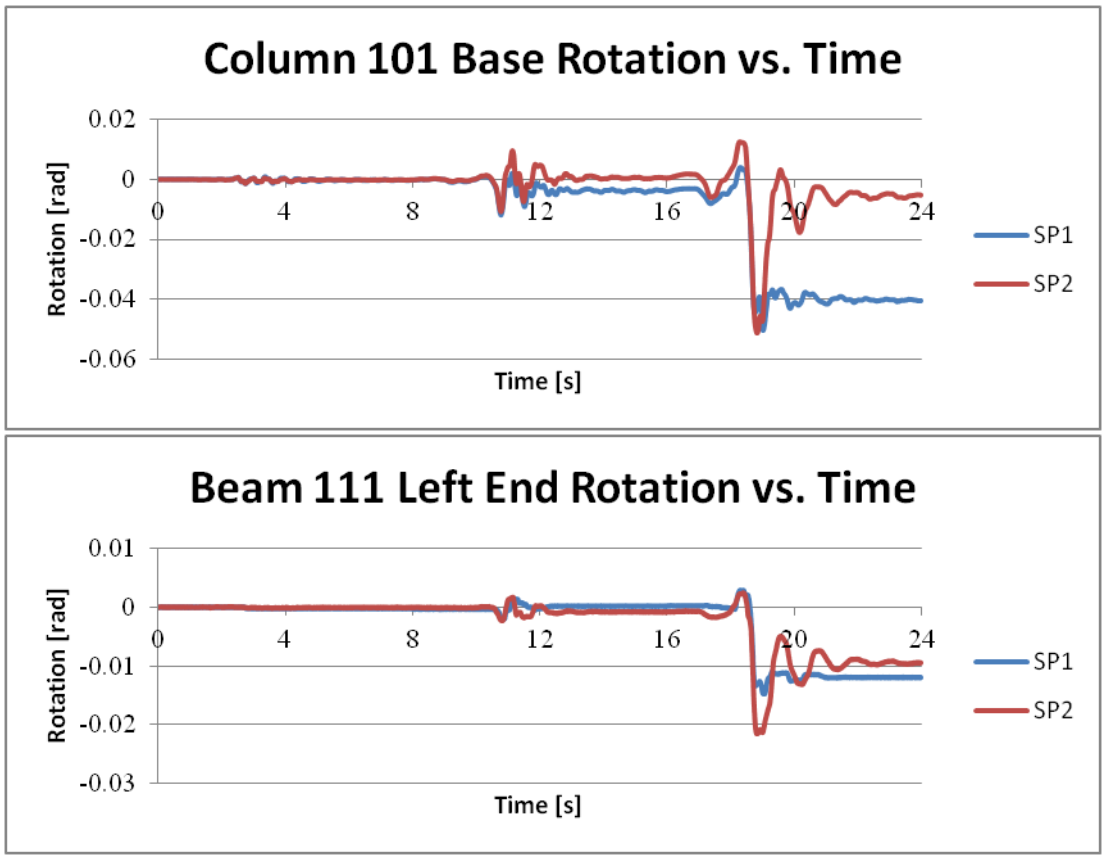

Figure 2. 19 Column 101 base and beam 111 left end rotation time history comparisons

Column 101's base rotation exhibits the same behaviour as the 1st storey drift response, where Specimen #2's residual is lesser than that of Specimen #1's. In the case of Beam 111's left end rotation, the residual values are relatively closer to each other, unlike Column 101's values, suggesting that the presence lap splices have a bigger influence on column behaviours.

3. NUMERICAL MODELS

3.1 General

The OpenSees Simulation Platform was used for generating the models (referred to as OS in tables and figures) of each specimen in order to estimate the seismic response of the test frames. The models were calibrated through the time history analyses results. The calibrated models were then used in pushover and time history performance assessments.

Beams and columns in the OpenSees models were modelled using force-based elements defined with nonlinear fibre sections at integration points. Second order geometric nonlinearity effects were considered in columns.

Formulation of the *Nonlinear Beam Column Element* elements follows the Euler-Bernoulli beam theory, which ignores shear deformations. For the joint regions, joint offsets were made at the element ends for both beam and column elements in accordance with the procedures defined in ASCE/SEI 41-06, as the fully rigid joint offsets suggested by TEC 2007 lead to an unreasonably low initial 1st mode period and did not provide results that matched the global response.

Most column rigid end zones were taken as zero in order to compensate for the effect of joint rotation on column stiffness as this system was a strong beam-weak column system. Beam lengths were defined from centerline to centerline of the adjacent columns. Shear deformations at the beam-column connection regions were neglected in the fibre frame models.

The concrete material model used in the OpenSees models was *Concrete01*, which is the uniaxial Kent and Park (1971) concrete material model with no tensile strength and degraded linear unloading/reloading stiffness as proposed by Karsan and Jirsa (1969). Through this material model, confinement effects of transverse reinforcement were accounted for by increasing the strength and strain capacities of the unconfined concrete in order to reflect the behaviour of the concrete in the confined zones, which have a residual stress associated with them.

For modelling the behavior of steel reinforcement, a stress-strain relation was defined using the *uniaxialMaterial ReinforcingSteel* command with 90% of the yield and ultimate strength values of the reinforcing steel obtained from material tests, to provide more realistic predictions of column strengths. An onset strain hardening value of 0.01 and an ultimate strain value of 0.1 was used, as suggested by TEC 2007. The *ReinforcingSteel* material model was created specifically for simulating reinforcing steel in a fibre section. A perfect bond between the concrete and steel was assumed in the models.

Dynamic properties of the specimens were modelled as lumped masses at the nodes with Rayleigh damping assumed for the time history analyses.

The *Static Pushover* analysis feature in OpenSees was used to simulate the frame's nonlinear static response to the ground motions. The *Dynamic Ground-Motion* analysis feature in OpenSees was used to simulate the frame's nonlinear dynamic response to the ground motions. The Krylov-Newton time-stepping algorithm was used to better capture any strength degradations.

Figure 3.1 presents an overview of the modelling strategy.

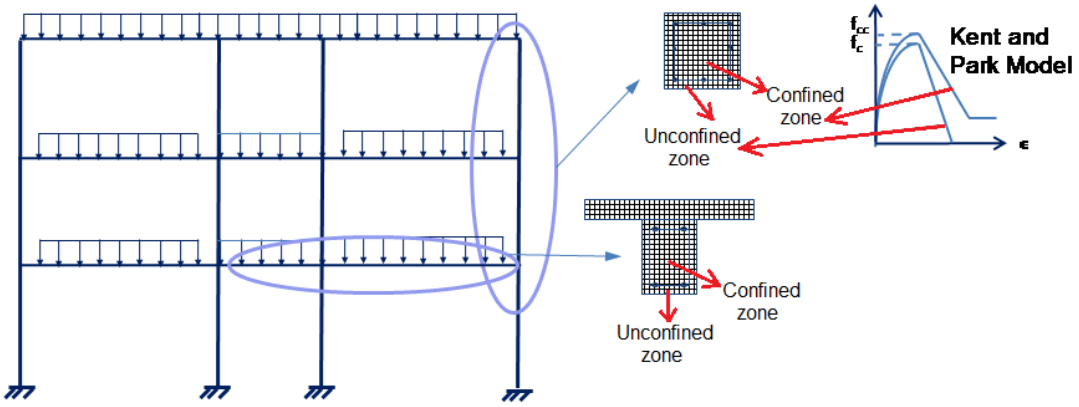

Figure 3. 1 OpenSees model with force-based elements

3.2 Specimen #1

The OpenSees models were calibrated with the observed behaviour of Specimen #1 and comparisons are made between the OpenSees and experimental results. Performance evaluations using these models were conducted following the procedures defined in TEC 2007 and ASCE/SEI 41-06.

The following global assumptions were made in order to calibrate the model's time history output to match the experimental results:

- Storeys were modelled as rigid diaphragms;
- Column rigid offsets were set as zero, except for the exterior joints at the 1st and 2nd storey, where the full dimension are defined;
- Beam rigid offsets were set as the full dimension, except for the exterior joints at the 1st and 2nd storey, where they were set as zero;
- Beam and column longitudinal reinforcement steel behaviour were defined separately;
- Concrete strengths at each floor were defined separately;
- Steel strengths in columns were 90% of the nominal values determined from the material tests;
- The force-based beam and column elements had 5 Gauss-Lobatto integration points;
- P-Delta effects were considered in the column elements;
- Dead loads were calculated from the weight of steel blocks (which represent the transverse beam and slab weight) and applied as uniformly distributed loads on the beams;
- Nodal masses for dynamic analyses were assigned with a dead load factor of 1.0, representative of the physical pseudo-dynamic test; and
- The damping value was set at 2.50% for stability purposes (discussed later)

The OpenSees model completes one time history analysis in less than a few minutes on a standard personal laptop computer and the post-processing for the models are fairly straight forward.

The resulting model for Specimen #1 contained 9 beam elements, 12 column elements, 16 nodes, and 48 degrees of freedom.

3.3 Specimen #1-Comparison with Experimental Results

The OpenSees model time history analysis results for Specimen #1 are presented here in comparison with the pseudo-dynamic results, as this was used to calibrate the model. The resulting model was used to conduct pushover and time history analyses for performance evaluations.

The initial 1st mode period from the OpenSees model was 0.48 seconds. The roof displacement time history comparison is shown in Figure 3.2. The inter-storey drift ratio time history comparisons are shown in Figure 3.3, and the shear force time history comparisons are shown in Figure 3.4.

The model does not predict peak displacements well during D1. Even though there are essentially no residuals in the physical test and the model, the 1st mode period suggests that the model is slightly stiffer and over-predicted the peak displacements (and forces). As seen in Figure 3.3, none of the 2nd and 3rd storey drift residuals are being captured accurately, although some peak values are.

The accuracy of the model was first evaluated through the global responses such as the peak roof displacement and peak base shear forces obtained during each successive ground motion. Error percentages for peak roof displacement and peak shear are presented in Table 3.1 and Table 3.2, respectively. However, the accuracy of numerical models should be evaluated in terms of inter-storey drift ratios and storey shear forces, as these comparisons capture the effects of higher modes better. These errors are presented in Table 3.3 and Table 3.4, respectively.

The OpenSees model also did not capture the behaviour during D3 accurately with regards to peaks or residual displacements. After approximately 18.5 seconds, the damages predicted in the models were too great and only accumulate in the 1st storey, leading to a soft-storey effect, which was not observed in the physical test. The specimen appears to have been stronger than expected, as beam mechanism formations and non-ductile flexural (no shear) failures were observed. Thus, the values in the model after 18.5 seconds were discarded in the error calculations and comparisons on local scales as they are not reliable due to the instability experienced in the system. A damping value of 2.50% was arbitrarily chosen as a value which allows the simulation to run until the very end of D3 ground motion. The damping value does not significantly affect the results during D1 and D2 ground motions.

It should be noted that extensive damages in the joint regions were observed during D3 for both specimens, and that a more detailed nonlinear spring element in this region could have been utilized in the model to better capture damage redistribution. The inability to capture residual drifts in the 2nd and 3rd storeys of the model could also be attributed to the fact that the model is only fixed at the 1st storey column bases, and lacks more detailed elements at the other joints which properly capture correct rotations. However, this was not done due to time constraints. This joint flexibility could have been a major factor in the uniform drifts observed in the test specimen as drift capacities are a function of many factors such as the amount of transverse reinforcement, shear stresses, and axial loads.

Another reason leading to these inaccurate predictions is the fact that the material models in the software program were created for simulating “quality” materials. The effects of the accumulated deficiencies affecting the drift capacities in the specimens were too great and not captured properly. Modelling materials in deficient systems by using nominal but reduced strength properties in hopes to predict accurate seismic responses is not very efficient. The main cause is the inability of modelling degradation during the ground motions. The errors in the model can be generally attributed to numerical errors.

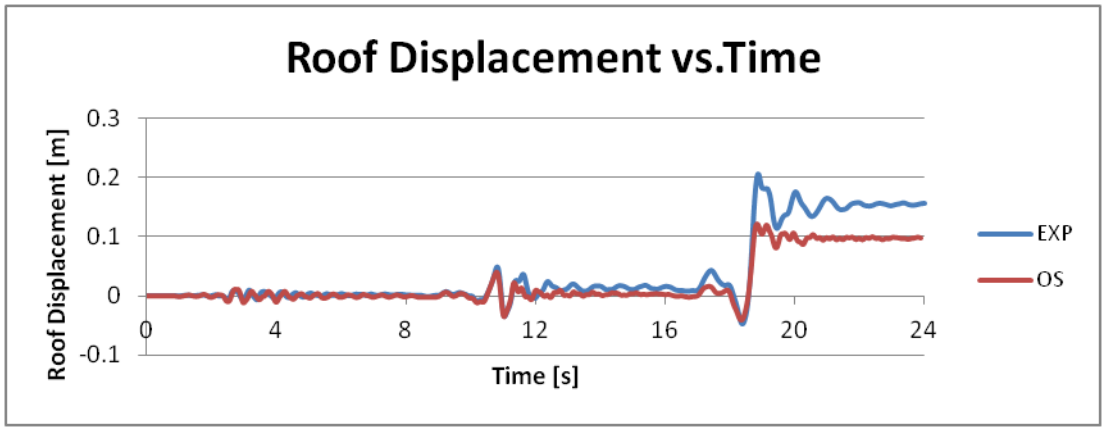

Figure 3. 2 Roof displacement time history comparison (SP1)

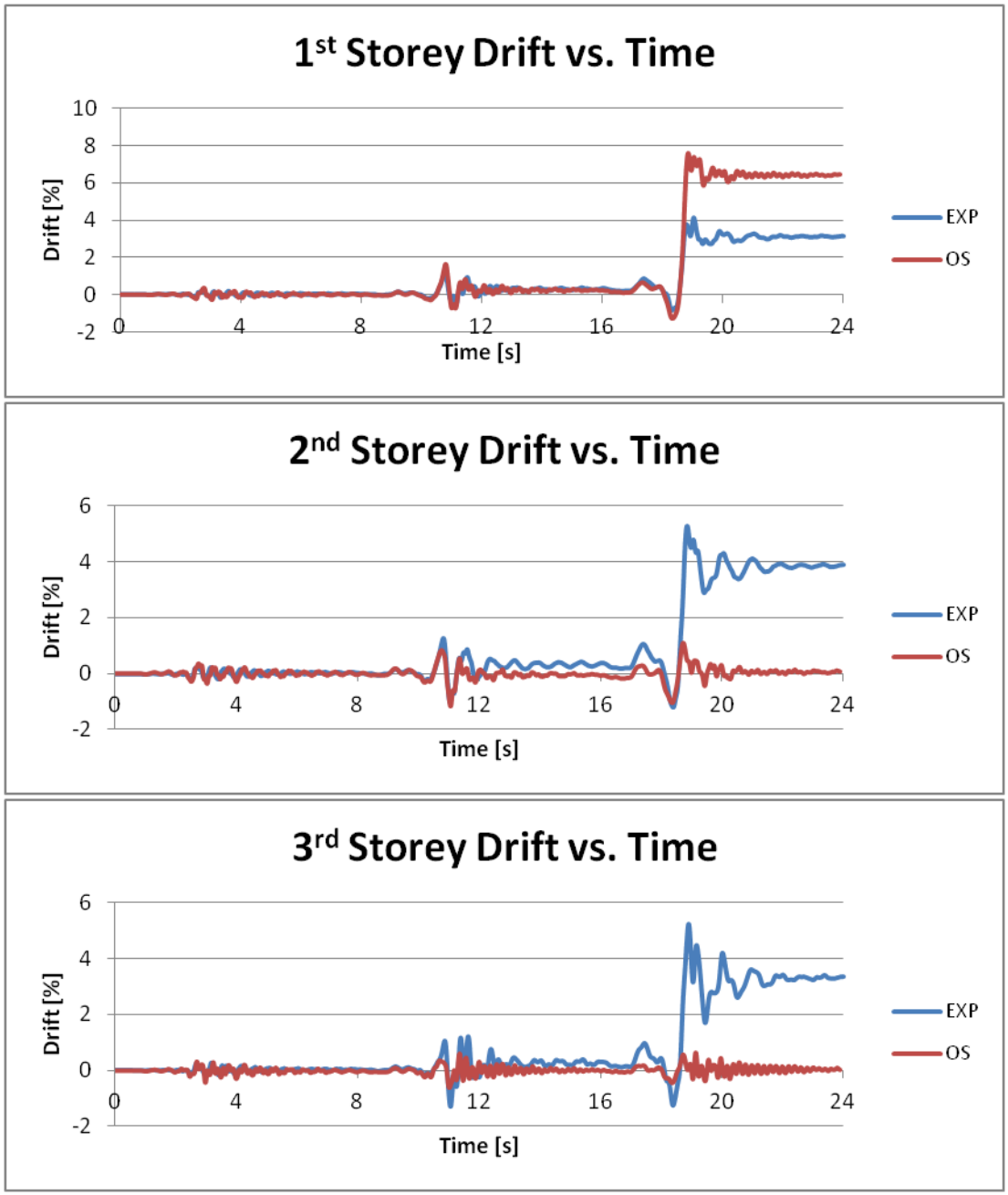

Figure 3. 3 Inter-storey drift ratio time history comparisons (SP1)

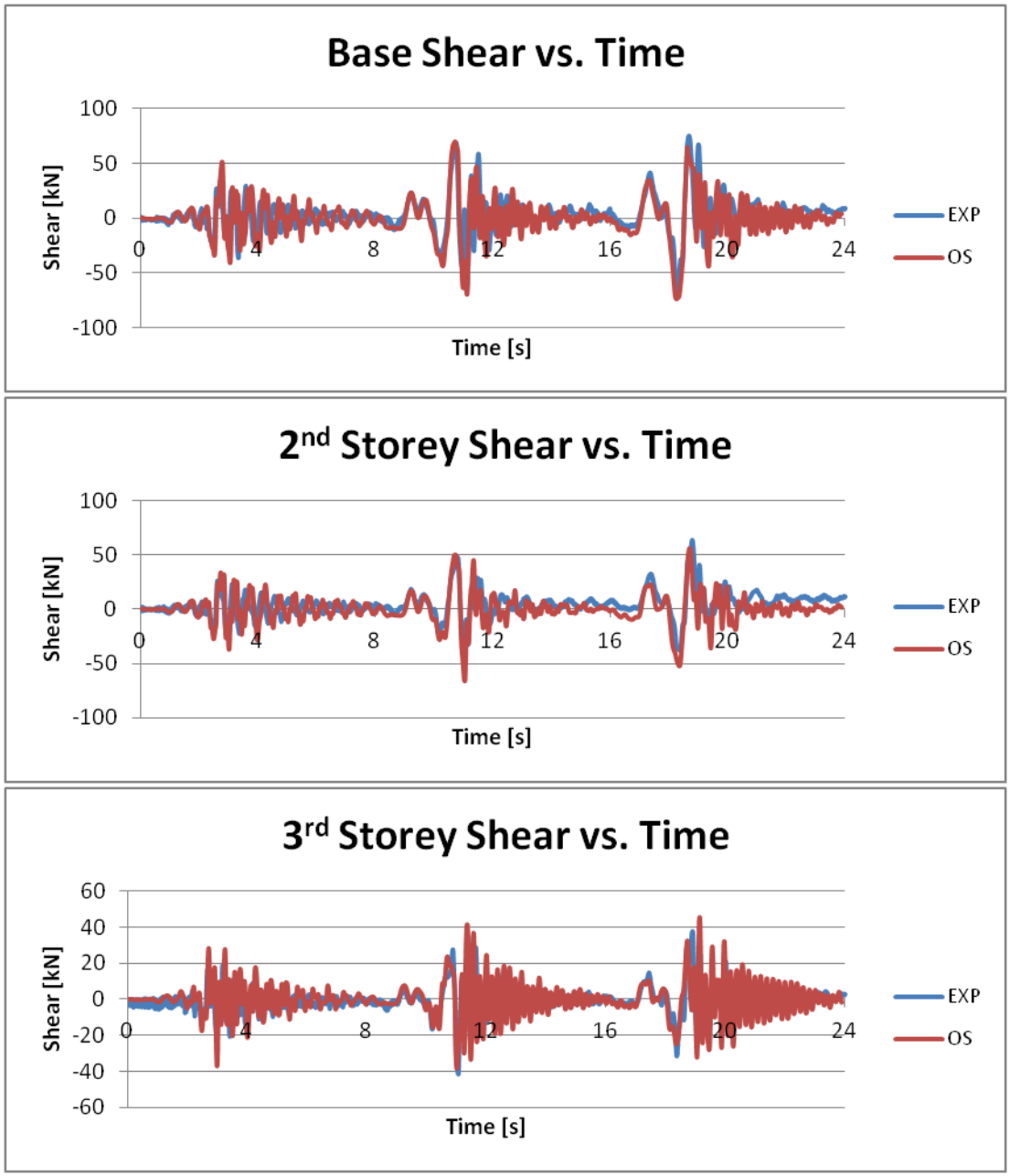

Figure 3. 4 Storey shear force time history comparisons (SP1)

It is clear that the model captures the storey shear forces better than the inter-storey drifts, indicating that it is more suitable for force-based assessments. Nonetheless, results of performance evaluations conducted using strain-based procedures of TEC 2007 and rotation-based procedures of ASCE/SEI 41-06 are presented in the chapter as this was one of the objectives set forth in this thesis study.

Table 3. 1 Peak roof displacement error (SP1)

Ground Motion	Maximum Roof Displacement [mm]		Error [%]
	Experiment	OpenSees	
D1	9.14	11.3	23.6
D2	35.6	41.2	15.7
D3	48.3	41.2	-14.7

Table 3. 2 Peak base shear error (SP1)

Ground Motion	Maximum Base Shear [kN]		Error [%]
	Experiment	OpenSees	
D1	36.5	41.1	12.6
D2	68.5	69.9	2.0
D3	66.6	74.1	11.3

Table 3. 3 Peak inter-storey drift error (SP1)

Storey	Ground Motion	Maximum Inter-Storey Drift [%]		Error [%]
		Experiment	OpenSees	
1st	D1	0.20	0.36	80.0
1st	D2	1.20	1.64	36.7
1st	D3	0.86	1.29	50.0
2nd	D1	0.23	0.35	52.2
2nd	D2	1.28	0.82	-35.9
2nd	D3	1.19	1.04	-12.6
3rd	D1	0.26	0.32	23.1
3rd	D2	1.20	0.60	-50.0
3rd	D3	1.27	0.43	-66.1

Table 3. 4 Peak storey shear error (SP1)

Storey	Ground Motion	Maximum Storey Shear [kN]		Error [%]
		Experiment	OpenSees	
1st	D1	36.5	41.1	12.6
1st	D2	68.5	69.9	2.0
1st	D3	66.6	74.1	11.3
2nd	D1	26.1	33.4	28.0
2nd	D2	47.9	49.8	4.0
2nd	D3	38.2	52.6	37.7
3rd	D1	18.8	28.1	49.5
3rd	D2	41.3	38.2	-7.5
3rd	D3	31.3	24.8	-20.8

As visible in Table 3.3, the 1st storey peak values are over-predicted in the model while the 2nd and 3rd storey values are under-predicted (with the exception of during D1 due to the inability to capture micro-cracks in the model). Due the formation of a first storey mechanism, the peaks in the 2nd and 3rd storeys are not captured as well as the 1st storey. In the 1st storey, error during D2 is less than those of D1 (due to energy dissipation) and D3 (due accumulated damages in the 1st storey). Therefore, the model is more stable and reliable during the intermediate D2 ground motion. As for the peak storey shear errors presented in Table 3.4, the model mostly over-predicts the values measured from the experiment, suggesting that full yielding of the steel does not occur during the pseudo-dynamic tests. Once again, the model results are most reliable in the 1st storey during D2.

The curvature time histories of the 1st storey column bases are presented in Figure 3.5, followed by the column tops in Figure 3.6 as these members are the most critical. It has been shown in the literature that force-based elements lose objectivity at the local (curvature) and/or global (element) scale, depending on the number of integration points used. Therefore, objective OpenSees results obtained using the geometric scaling factors proposed by Coleman and Spacone (2001) are compared with the experimental results. Up until the point of approximately 18.5 seconds, the analysis results are in general agreement with the experimental curvature demands. The convention for curvature is positive in the counter-clockwise direction.

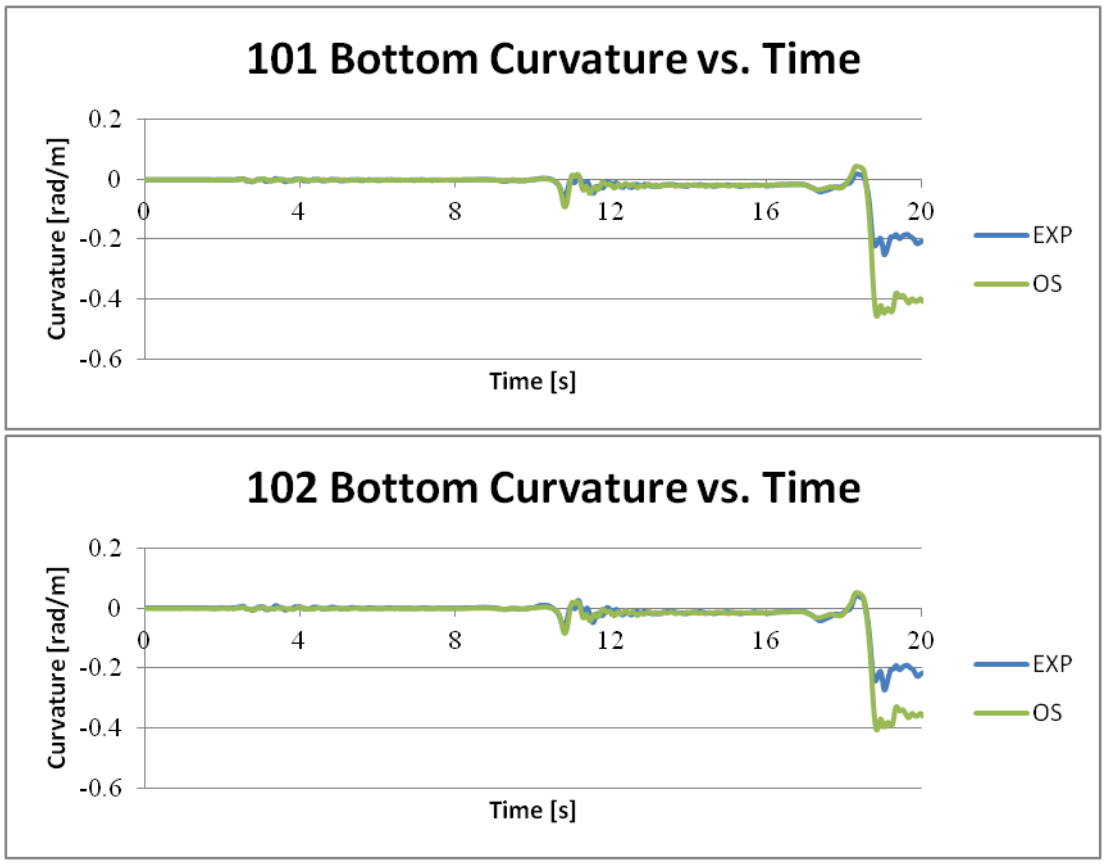

Figure 3. 5 Comparisons of bottom end curvatures of 1st storey columns (SP1)

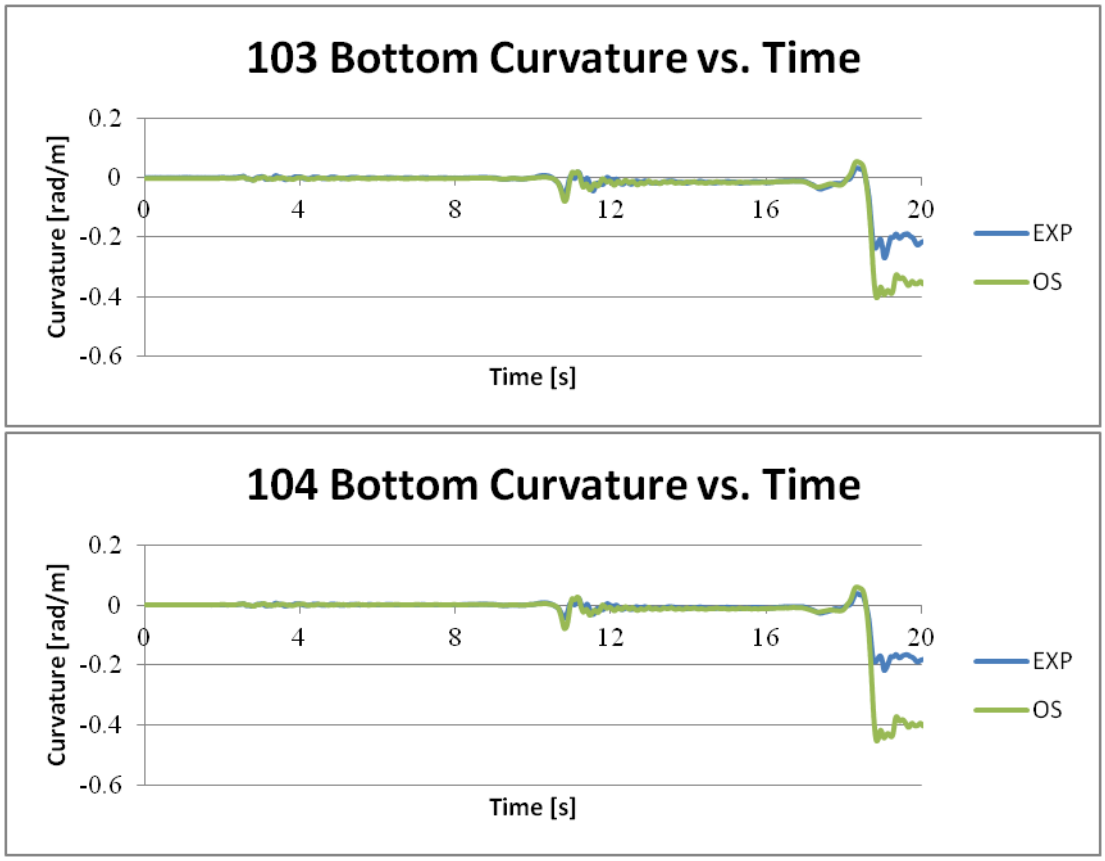

Figure 3.5 (Continued)

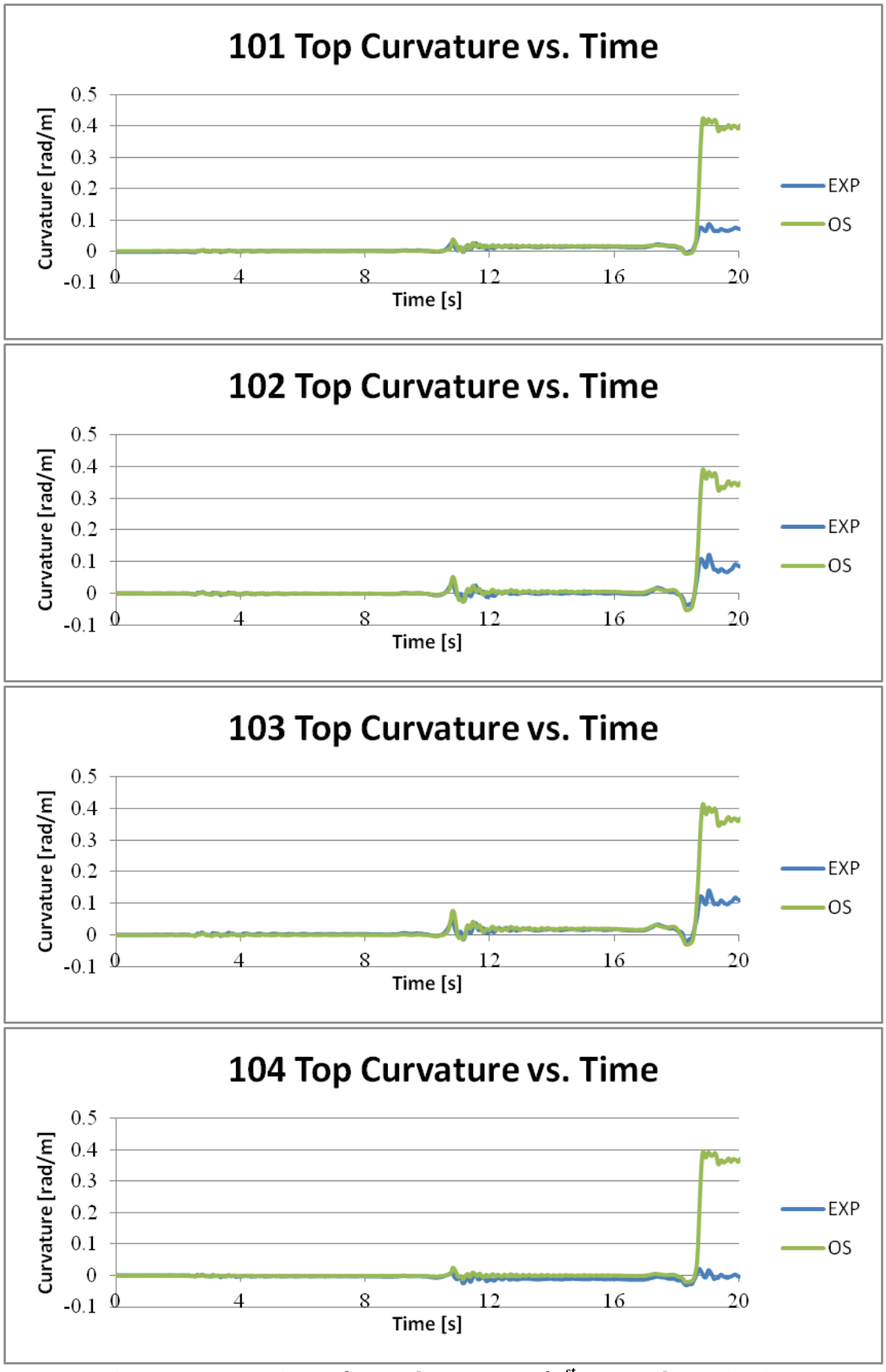

Figure 3. 6 Comparisons of top end curvatures of 1st storey columns (SP1)

Peak and residual values during D2 are captured quite well, indicating that the results at the local level are also reliable. As discussed earlier, the model is unstable during D3 after approximately 18.5 seconds, which is apparent from the over-predicted curvatures at both ends of all members. Another important observation is that in the experiment, the top residual curvatures are considerably less than those measured at the bottoms during D3. The OpenSees model does not capture this phenomenon and predicts the same residual values for the top and bottoms of the elements. Thus, this is another indication that predictions from the model during D3 are not reliable.

3.4 Specimen #2

Similar to Specimen #1, Specimen #2's OpenSees model uses force-based elements with the same material models.

As this specimen had lap splices, separate elements were created in the spliced regions to account for the extra reinforcement. However, these splice lengths did not conform to the $40d_b$ length as required by TEC 2007 (only 75% of this length was provided). To account for this deficiency, the yield strength reduction in the model for these spliced-region elements were reduced linearly, as suggested by TEC 2007 and exponentially, as suggested by ASCE/SEI 41-06.

Dynamic properties of the specimens were modelled as lumped masses at the nodes with a 2.51% (for TEC 2007) and 2.44% (for ASCE/SEI 41-06) Rayleigh damping assumed for the time history analyses for stability purposes, as previously discussed.

The resulting model contained 9 beam elements, 24 column elements, 28 nodes, and 84 degrees of freedom.

The following global assumptions were made as to match, as closely as possible, the calibration of Specimen #1's model:

- Storeys were modelled as rigid diaphragms;
- Column rigid offsets were set as zero, except for the exterior joints at the 1st and 2nd storey, where the full dimension are defined;
- Beam rigid offsets were set as the full dimension, except for the exterior joints at the 1st and 2nd storey, where they were set as zero;
- Beam and column longitudinal reinforcement steel behaviour were defined separately;
- Concrete strengths at each floor were defined separately;
- Steel strengths in columns were 90% of the nominal values determined from the material tests;
- The force-based beam and column elements had 5 Gauss-Lobatto integration points and the spliced-region elements had 2 Gauss-Lobatto integration points;
- P-Delta effects were considered in the column elements;
- Dead loads were calculated from the weight of steel blocks (which represent the transverse beam and slab weight) and applied as uniformly distributed loads on the beams; and
- Nodal masses for dynamic analyses were assigned with a dead load factor of 1.0, representative of the physical pseudo-dynamic test

3.5 Specimen #2-Comparison with Experimental Results

The OpenSees model time history analysis results are presented here in comparison with the respective pseudo-dynamic results. The resulting models were used to conduct pushover and time history analysis performance evaluations.

The initial 1st mode period from the OpenSees model was 0.46 seconds, slightly less than that of Specimen #1.

The roof displacement time history comparison is shown in Figure 3.7. The inter-storey drift ratio time history comparisons are shown in Figure 3.8, and the shear force time history comparisons are shown Figure 3.9.

The accuracy of the model was first evaluated through the global responses such as the peak roof displacement and peak base shear forces obtained during each successive ground motion. Error percentages for peak roof displacement and peak shear are presented in Table 3.5 and Table 3.6, respectively.

As mentioned, the accuracy of numerical models should be evaluated in terms of inter-storey drift ratios and storey shear forces as these comparisons capture the effects of higher modes better. These errors are presented in Table 3.7 and Table 3.8, respectively.

It is worth mentioning here that any output from the model associated with forces do not differ significantly for the two different definitions of yield strength (referred to as TEC and ASCE in tables and figures) in the lap-spliced elements.

Once again, the OpenSees model did not capture the behaviour during D1 or D3 accurately when comparing the peak or residual displacements. After approximately 18.5 seconds during D3, the damages predicted in the models were too great and only accumulated in the 1st storey, leading to the soft storey effect which was not observed in the physical test. Thus, the values after this time are discarded in the error calculations and comparisons on local scales as they are not reliable due to the instability experienced in the system. Columns with lap splice deficiencies in computer models are sensitive to the plastic hinge length (which is assumed), splice length, concrete strength, and axial load levels, as observed by Binici and Mosalam (2007).

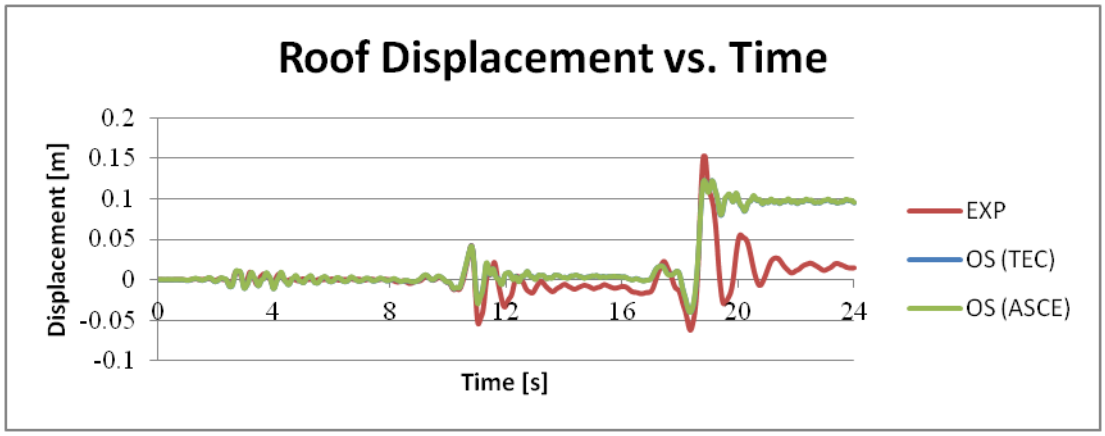

Figure 3. 7 Roof displacement time history comparison (SP2)

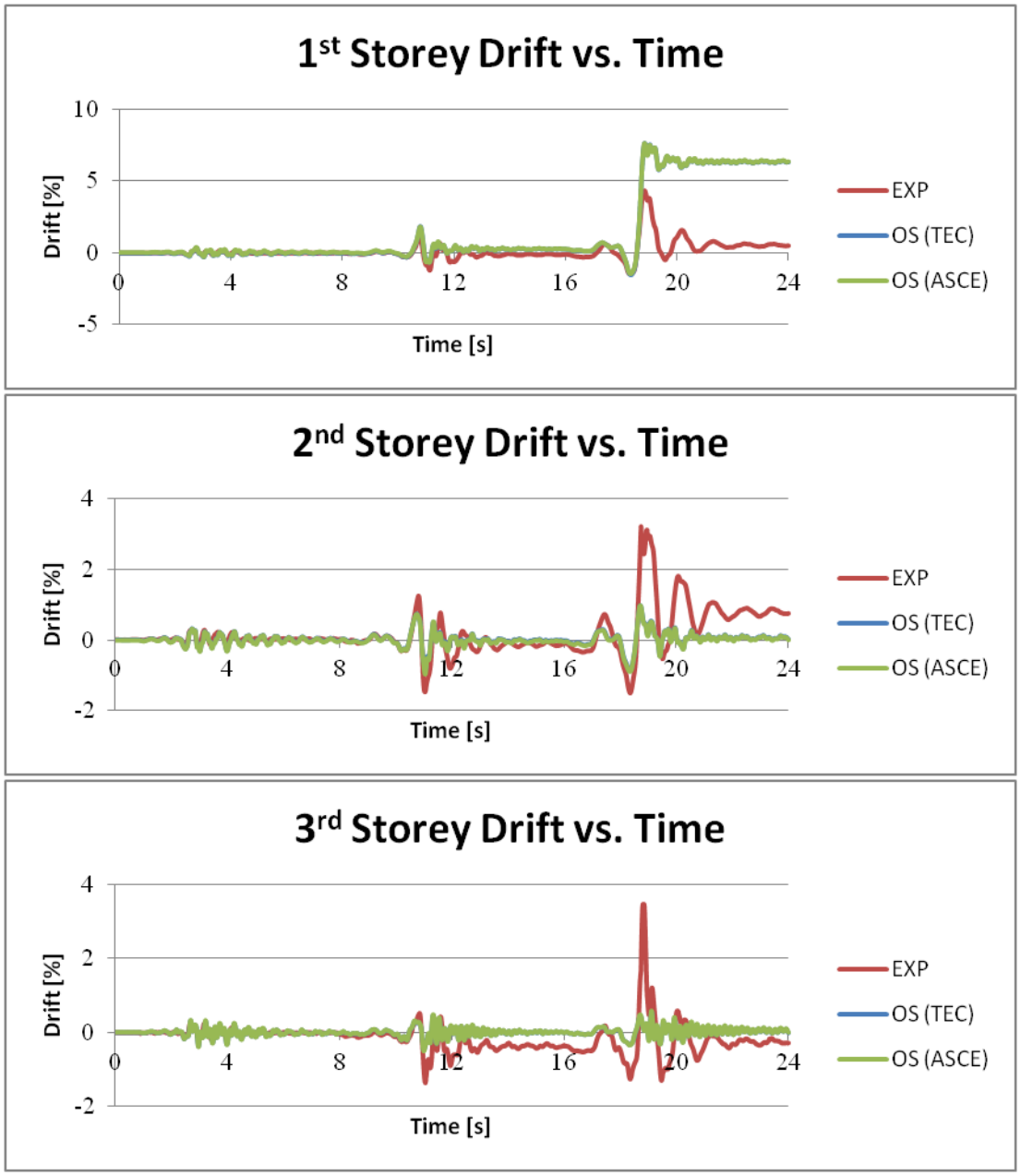

Figure 3. 8 Inter-storey drift ratio time history comparisons (SP2)

It should be noted here again that extensive damages in the joint regions were observed during D3 for both specimens, and that unless joint deformations are explicitly accounted for, local deformations such as end rotations cannot be captured. In general, estimating seismic responses on a local scale is an extremely challenging, if not impossible, task.

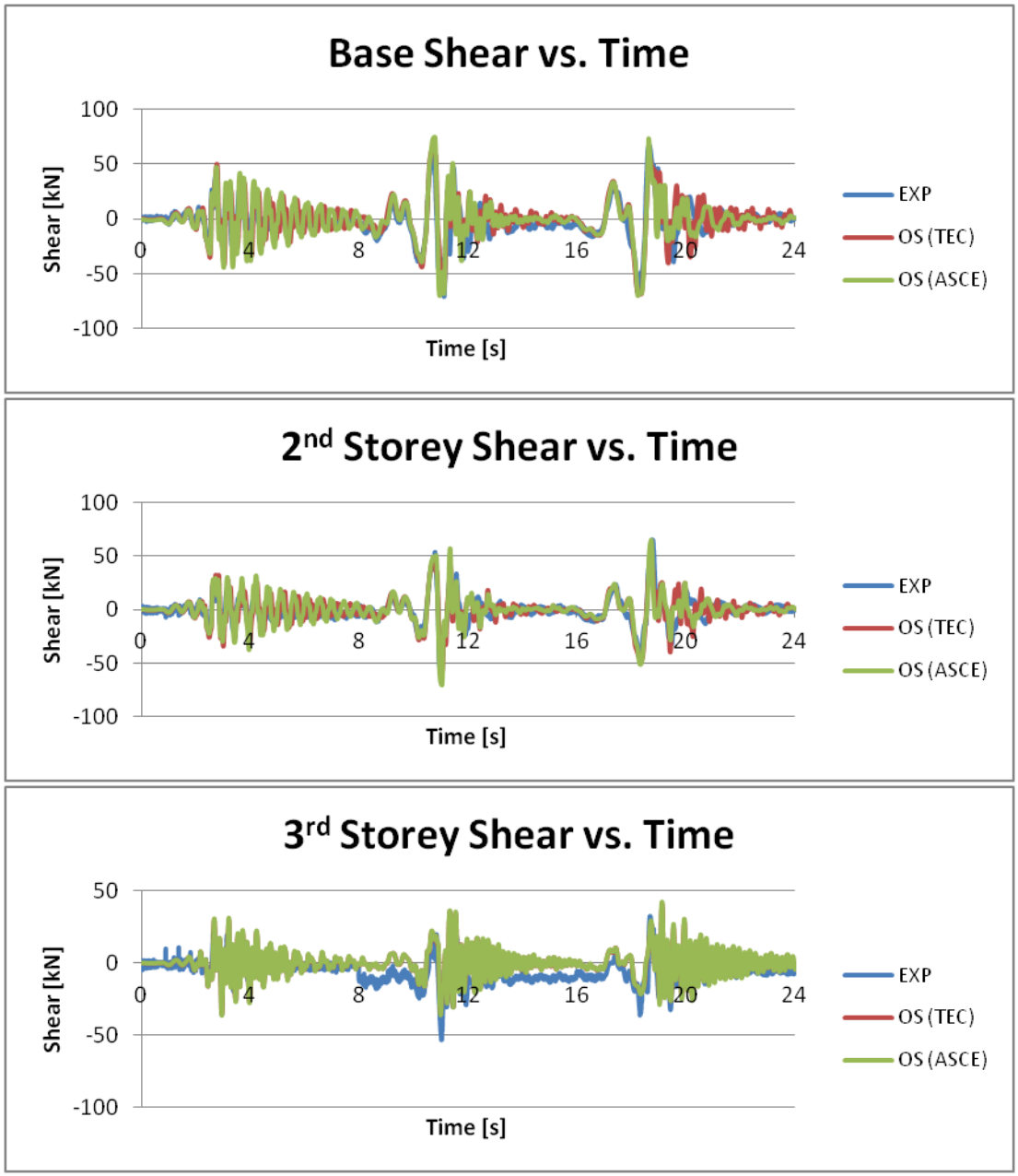

Figure 3. 9 Storey shear force time history comparisons (SP2)

Table 3. 5 Peak roof displacement error (SP2)

Ground Motion	Maximum Roof Displacement [mm]			Error [%]	
	Experiment	OS (TEC)	OS (ASCE)	OS (TEC)	OS (ASCE)
D1	9.3	11.0	11.1	18.3	19.4
D2	55.0	42.1	41.2	-23.5	-25.1
D3	62.7	40.6	40.8	-35.2	-34.9

Table 3. 6 Peak base shear error (SP2)

Ground Motion	Maximum Base Shear [kN]			Error [%]	
	Experiment	OS (TEC)	OS (ASCE)	OS (TEC)	OS (ASCE)
D1	38.3	54.0	54.2	41.0	41.5
D2	70.9	75.9	77.8	7.1	9.7
D3	66.0	78.9	79.9	19.5	21.1

Table 3. 7 Peak inter-storey drift error (SP2)

Storey	Ground Motion	Maximum Inter-Storey Drift [%]			Error [%]	
		Experiment	OS (TEC)	OS (ASCE)	OS (TEC)	OS (ASCE)
1st	D1	0.24	0.36	0.36	50.0	50.0
1st	D2	1.19	0.64	0.70	-46.2	-46.2
1st	D3	1.44	1.53	1.49	6.3	3.5
2nd	D1	0.27	0.32	0.32	18.5	18.5
2nd	D2	1.48	0.88	0.97	-40.5	-34.5
2nd	D3	1.52	0.85	0.89	-44.1	-41.4
3rd	D1	0.24	0.32	0.32	33.3	33.3
3rd	D2	1.36	0.47	0.50	-65.4	-63.2
3rd	D3	1.25	0.33	0.34	-73.6	-72.8

Table 3. 8 Peak storey shear error (SP2)

Storey	Ground Motion	Maximum Storey Shear [kN]			Error [%]	
		Experiment	OS (TEC)	OS (ASCE)	OS (TEC)	OS (ASCE)
1st	D1	38.3	49.6	50.6	29.5	32.1
1st	D2	70.9	61.8	64.1	-12.8	-9.6
1st	D3	66.0	68.9	70.2	4.4	6.4
2nd	D1	23.0	32.3	32.6	40.4	41.7
2nd	D2	57.0	57.5	61.1	0.9	7.2
2nd	D3	49.8	47.0	48.4	-5.6	-2.8
3rd	D1	21.4	30.3	31.1	41.6	45.3
3rd	D2	53.2	34.7	36.2	-34.8	-32.0
3rd	D3	36.1	20.9	21.6	-42.1	-40.2

It is evident from Table 3.7 that Specimen #2's models are not as reliable from a displacement-based perspective. It should be reminded that a first storey mechanism was also predicted in these models, which was misrepresentative of the behaviour during the pseudo-dynamic test. However, the peak storey shear errors presented in Table 3.8 suggests that the models are more reliable during D2, the intermediate ground motion.

The curvature time history of the 1st storey column bases are presented in Figure 3.10, followed by the column top curvatures in Figure 3.11. Up until the point of approximately 18.5 seconds, the analysis results are in general agreement with the experimental curvature demands.

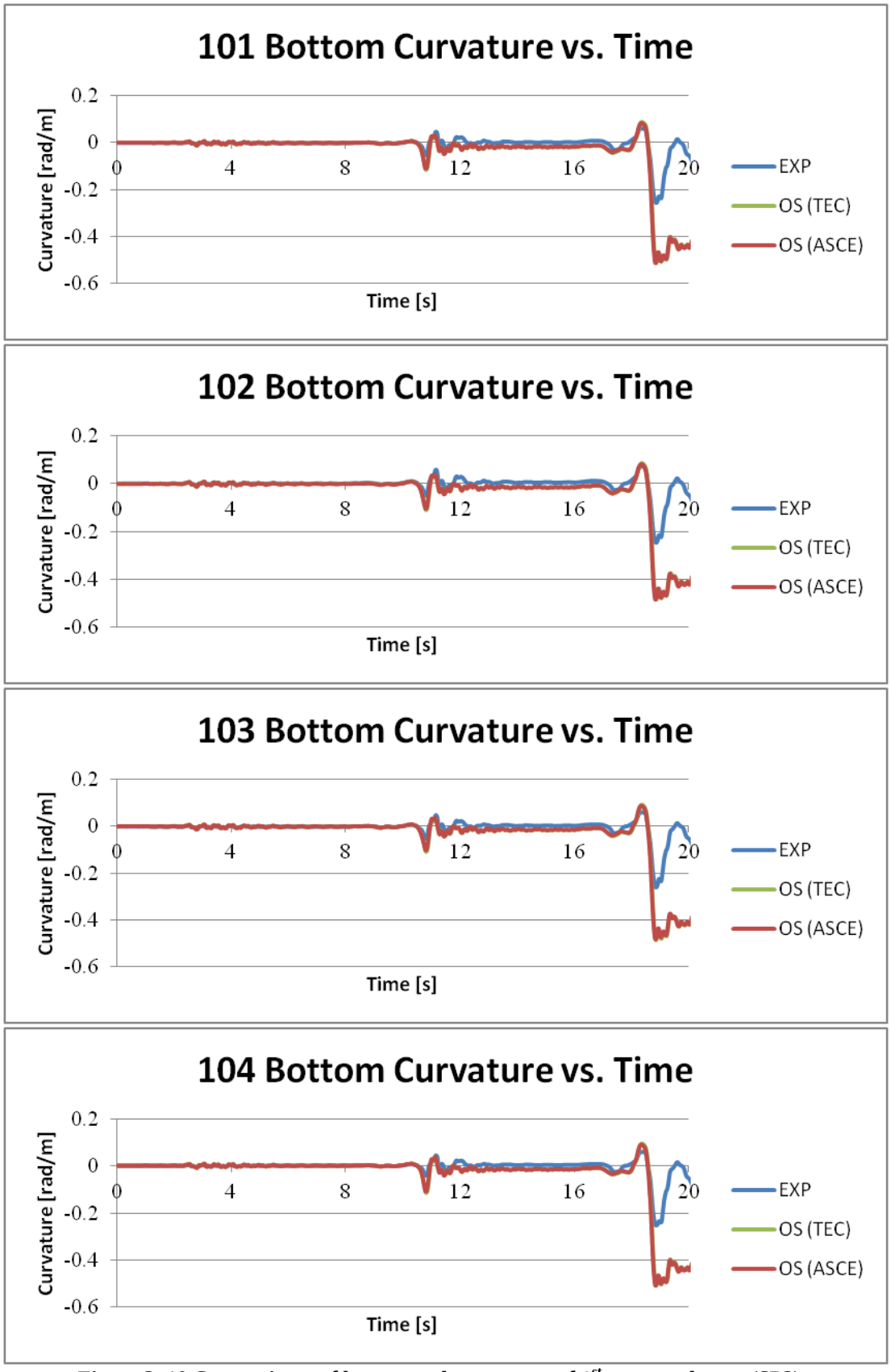

Figure 3. 10 Comparisons of bottom end curvatures of 1st storey columns (SP2)

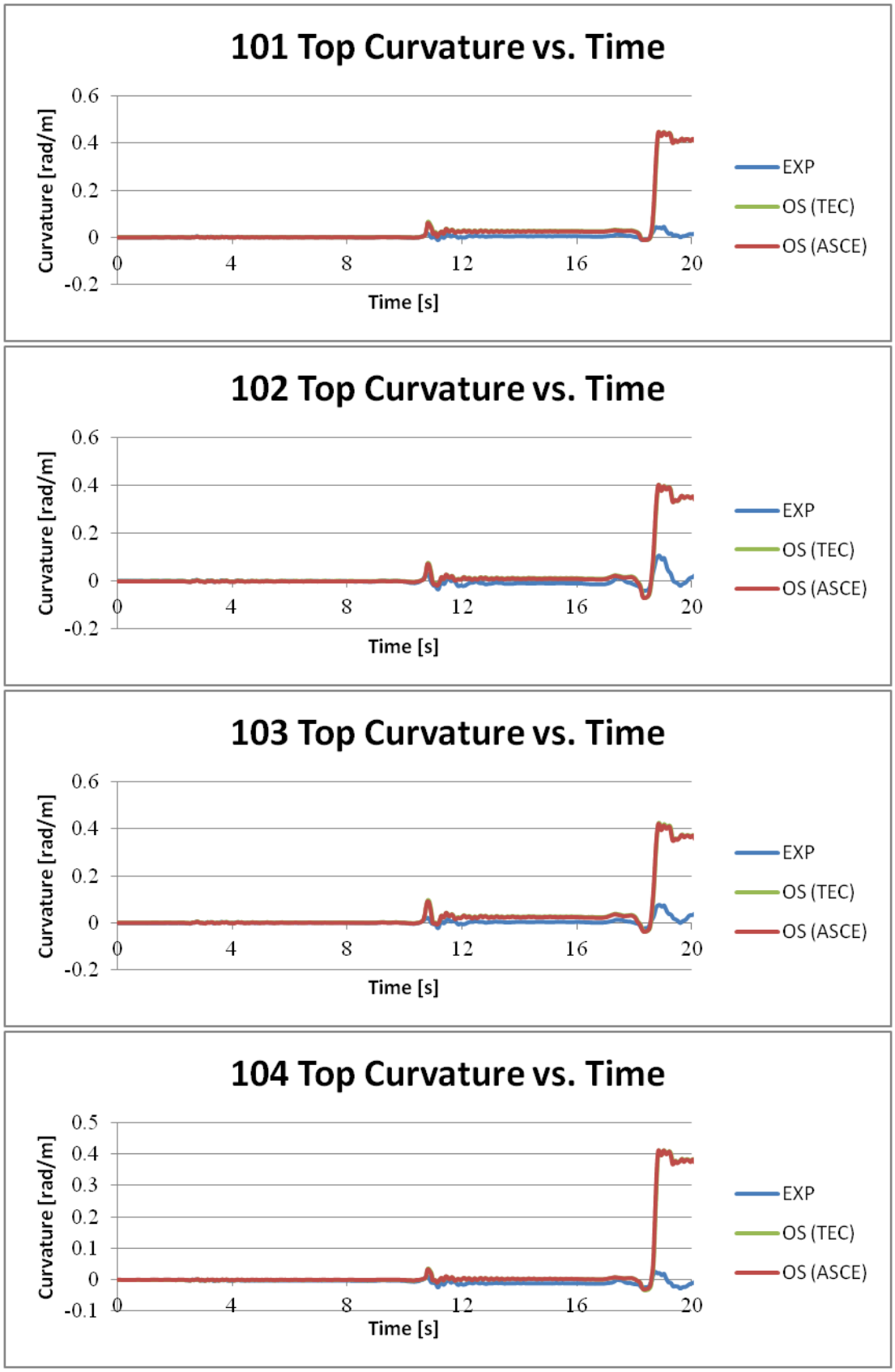

Figure 3. 11 Comparisons of top end curvatures of 1st storey columns (SP2)

Peak and residual curvatures during D2 are captured quite well, indicating that the results at the local level are reliable. As discussed earlier, the model is unstable during D3 after approximately 18.5 seconds, which is apparent from the over-predicted curvatures at both ends of all members. Another important observation is that in the experiment, the top residual curvatures are less than those measured at the bottoms, which the OpenSees models for this specimen do capture.

The presence of deficient lap splice lengths (75% of the $40d_b$ required by TEC 2007) in the case of a deficient frame does not affect the overall response, or change the failure mode. Therefore, TEC 2007's requirements for lap splice lengths can be seen as quite conservative and is able to tolerate deficiencies up to 25% of the required length. At both the global and local scale, it appears that TEC 2007 and ASCE/SEI 41-06's definition to account for lap splices do not yield significantly different results.

The author recognizes that certain researchers such as Dazio and Yazgan (2011) have proposed evaluation procedures based on the permanent residual displacements of a computer model simulation. However, since this model is not sophisticated enough to capture these residuals, performance evaluations will be conducted based on peak displacements.

3.6 Performance Evaluation of Test Frames

Performance levels of column elements have been assessed in accordance with the strain-based damage state limits given in TEC 2007 and the rotation-based performance limits given in ASCE/SEI 41-06. These evaluations were conducted by using the experimental measurement readings as well as the pushover and time history analysis results of the OpenSees models. Selected column member ends were also subjected to visual assessments for comparison purposes. It is important to note here that only the 1st and 2nd storeys during the pseudo-dynamic tests had LVDTs.

Three damage state limits for performance evaluations were defined for ductile members at the member level, according to TEC 2007: Minimum Damage (MD), Safety Limit (SL), and Collapse Limit (CL). Three performance limits for performance evaluations were defined for ductile members at the member level, according to ASCE/SEI 41-06: Immediate Occupancy (IO), Life Safety (LS), and Collapse Prevention (CP). Columns in both specimens satisfied the conditions in TEC 2007 for ductile behaviour. The strain limits in TEC 2007 for the longitudinal reinforcement and concrete in compression are presented in Table 3.9.

Table 3. 9 TEC damage state limits

	Strain Limits		
	MD	SL	CL
Longitudinal Reinforcement	0.010	0.040	0.060
Concrete (Compression)	0.0035	$0.0035+0.01(\rho_s/\rho_{sm})$	$0.004+0.014(\rho_s/\rho_{sm})$

where ρ_s is the volume of existing confining steel, ρ_{sm} is the volume of required confining steel, and the ratio ρ_s/ρ_{sm} has an upper bound of 1.0. The ρ_s/ρ_{sm} ratio was 0.33 for the columns.

The plastic rotation limits for the columns, which were bi-linearly interpolated from the axial load (formula 3.1) and shear reinforcement (formula 3.2) factor limits in ASCE/SEI 41-06's Table 6-8, are presented in Table 3.10.

$$\frac{P}{A_g f'_c} \tag{3.1}$$

$$\frac{A_v}{b_w s} \tag{3.2}$$

Table 3. 10 ASCE performance limits

Column	Plastic Rotation Limits [rad]		
	IO	LS	CP
Inner	0.0043	0.0101	0.0120
Outer	0.0048	0.0117	0.0140

These limits were used to assess the values obtained from the experiments and the OpenSees models along the plastic hinge length defined before, based on the assumption of uniform strain distribution along this region.

Figure 3.12 shows the damage state/performance limits and damage regions specified in TEC 2007 and ASCE/SEI 41-06, where the damage regions are:

- Minimum Damage (MD);
- Significant Damage (SD);
- Heavy Damage (HD); and
- Collapse (CP)

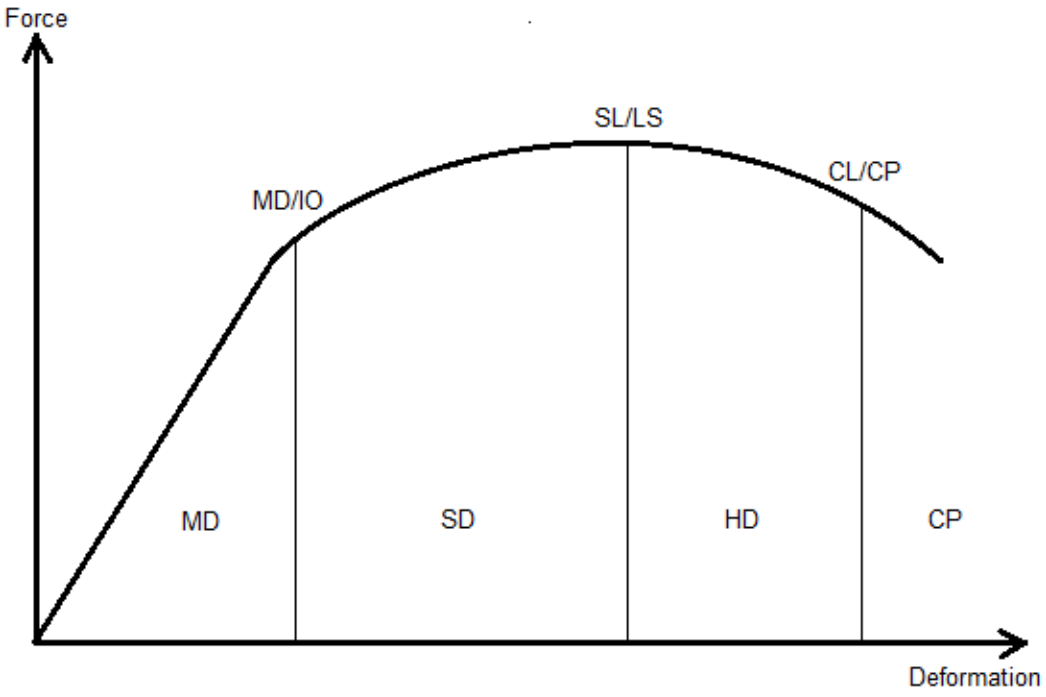

Figure 3. 12 Damage/performance limits and performance levels

3.6.1 Pushover and Time History Analysis Procedures

Using the pushover capacity curves, inelastic deformations (target displacements) were estimated through procedures defined in TEC 2007. This method relies on reducing the given multi-degree of freedom (MDOF) system to an equivalent single degree of freedom system (SDOF).
The procedure is as follows:

- Obtain the pushover capacity curve of the MDOF system
- Convert the capacity curve to the acceleration-displacement response spectrum (ADRS) format
- Convert the response spectrum to a demand curve in the ADSR format
- Plot the demand and capacity in the ADSR format on the same graph
- Determine the displacement demand of the SDOF system
- Convert the displacement demand computed in the previous step to the global roof displacement of the MDOF system

One main assumption affects the reliability of this method: The lateral load distribution is fixed and based on only the first mode of the elastic MDOF system.

For the time history analyses, strain and rotation values of member ends were extracted at the peak roof displacements of each ground motion.

The performance evaluation limits for each specimen were also compared with the observed damages from the pseudo-dynamic tests. The observed damages were assessed as objectively as possible as the goal of these evaluations is to compare the methods in TEC 2007 and ASCE/SEI 41-06 with the physical damages observed in the laboratory. The model did not capture the behaviour during D1 and D3 accurately due to the fact that D1 is too weak and D3 brings the system to collapse. Therefore, performance evaluations strictly focus on the D2 ground motion. It should be reminded again that the focus of this study is on the column members and the effects of the presence of deficient lap splices.

3.6.2 Specimen #1 Performance Evaluations

Performance evaluations of Specimen #1 are given in Figure 3.13 and Figure 3.14, based on the experimental values, for TEC 2007 and ASCE/SEI 41-06's limits, respectively.

During D2, the experimental values predicted most column member ends to be in the MD performance level, with some member ends in the SD performance level for TEC 2007's strain-based assessment (Figure 3.13). ASCE/SEI 41-06's rotation-based assessment (Figure 3.14) predicted all column member ends to be in the MD performance level.

Figure 3. 13 Specimen #1 performance evaluation w.r.t. TEC damage state levels (experimental peak demands)

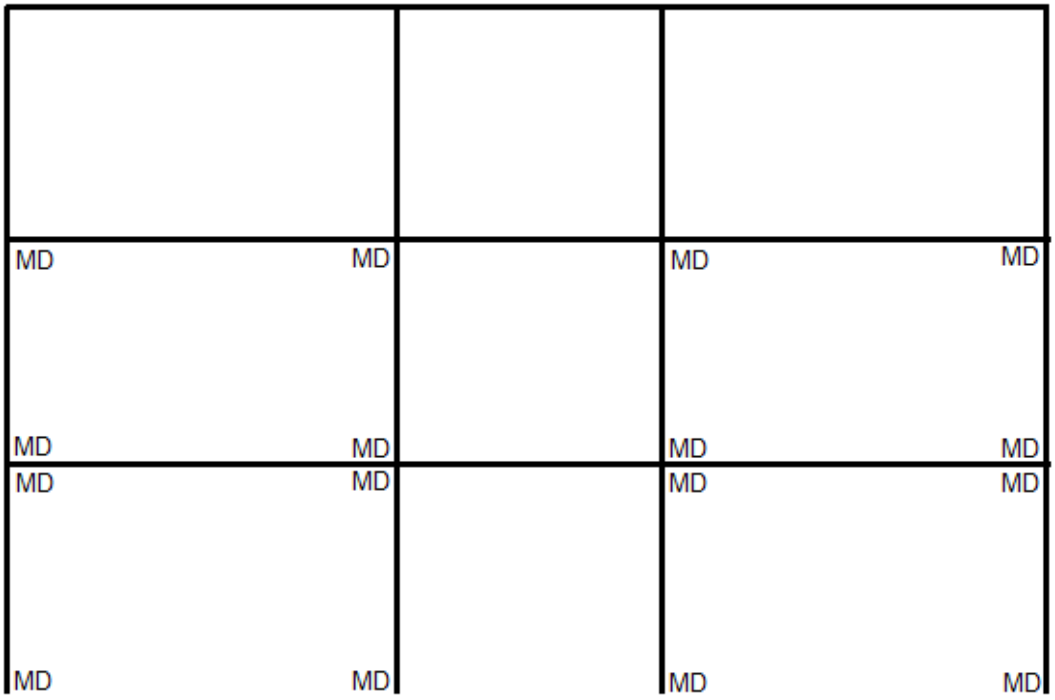

Figure 3. 14 Specimen #1 performance evaluation w.r.t. ASCE performance levels (experimental peak demands)

Performance evaluations of Specimen #1 are given in Figure 3.15 and Figure 3.16, based on the time history values, for TEC 2007 and ASCE/SEI 41-06's limits, respectively.

For the OpenSees time history values, almost all 1st storey column bottom ends were predicted to be in the SD performance level through TEC 2007's assessment (Figure 3.15), much like the corresponding TEC 2007 assessment for the experimental values (Figure 3.13). Almost all column ends in the 2nd storey are in the MD performance level for both experimental and time history assessments.

For the same time history results, almost all column member ends are predicted to be in the MD performance level through ASCE/SEI 41-06's assessment (Figure 3.16), with the exception of the 1st storey column bottom ends. The estimated performance levels were more conservative compared to the corresponding ASCE/SEI 41-06 assessment using the experimental values (Figure 3.14).

During this ground motion in the physical test, flexural macro-cracks were visible at the 1st storey columns and experimental results indicate that inelastic deformations occurred in the frame. Therefore, it is concluded that the only performance evaluation which did not match what was observed in the pseudo-dynamic test was ASCE/SEI 41-06's evaluation using experimental values. That particular ASCE/SEI 41-06 evaluation predicted minimum damages at every column member end. Figure 3.17 shows the damages at columns where significant damages were predicted by TEC 2007's assessments.

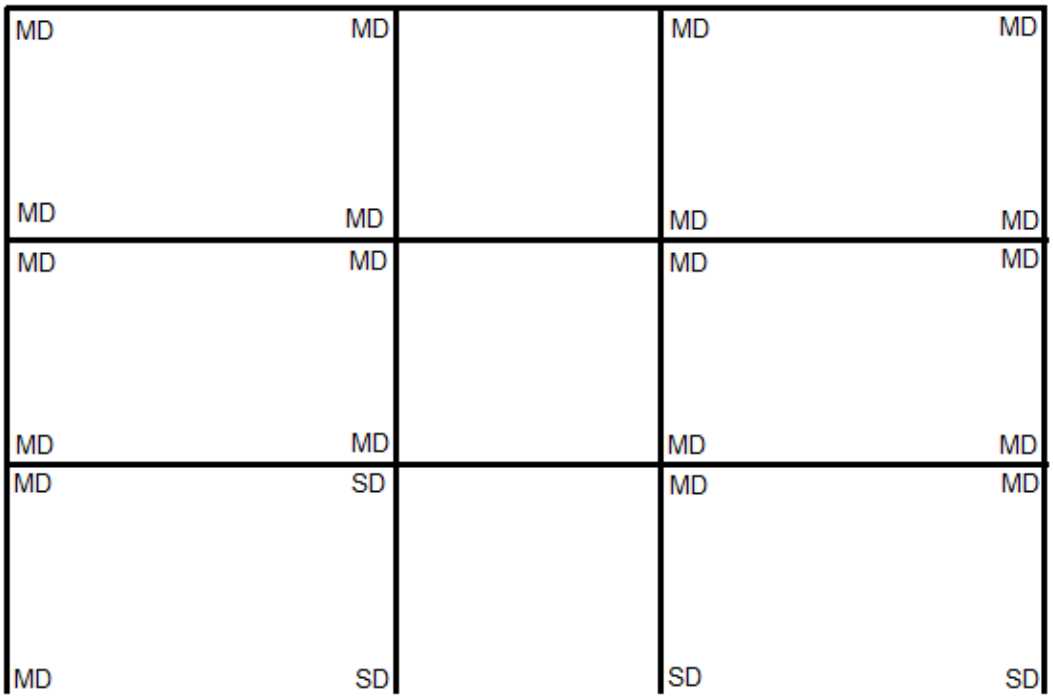

Figure 3. 15 Specimen #1 performance evaluation w.r.t. TEC damage state levels (time history peak demands)

Figure 3. 16 Specimen #1 performance evaluation w.r.t. ASCE performance levels (time history peak demands)

Figure 3. 17 Specimen #1 1st storey column damages during D2

A pushover analysis evaluation was not done due to the fact that the OpenSees model did not properly capture sufficient post-peak behaviour in the capacity curve. Convergence and stability problems arose shortly after the peak base shear was experienced by the system. Therefore, there is no available data at the target displacement calculated from the pushover analysis procedure. The capacity curve and with all 3 demands for Specimen #1 is shown in Figure 3.18.

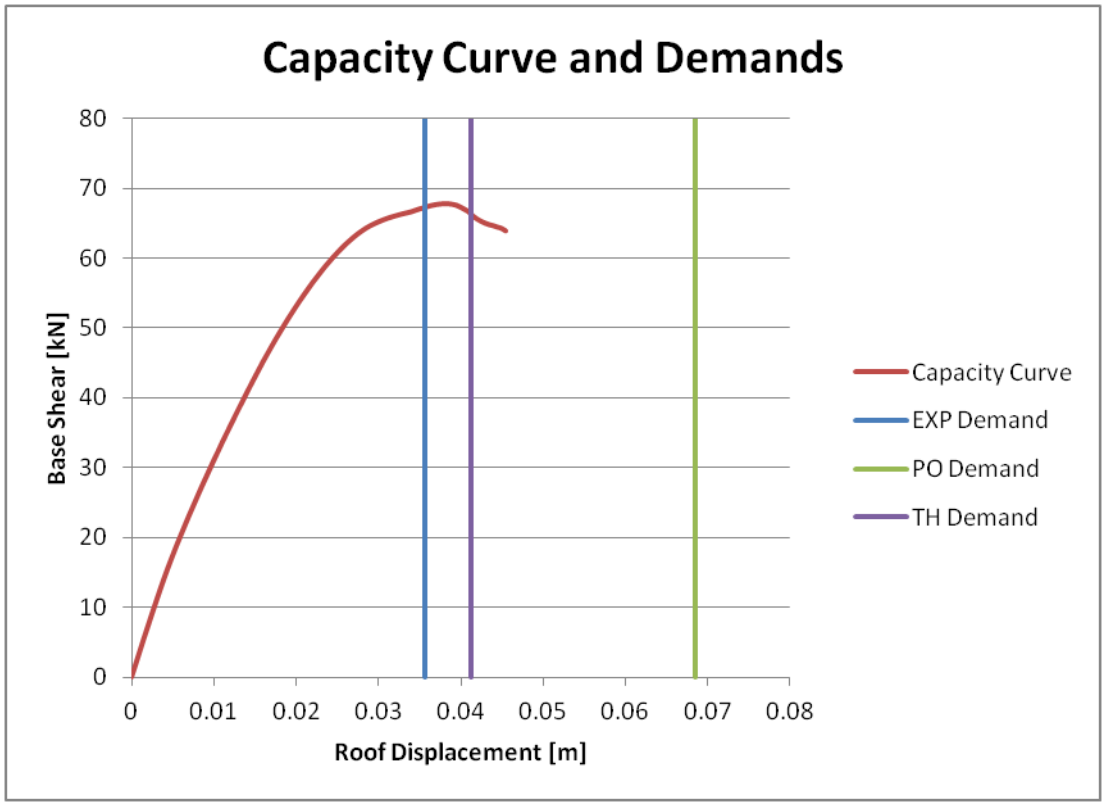

Figure 3. 18 Specimen #1 capacity curve and demands

3.6.3 Specimen #2 Performance Evaluations

Performance evaluations of Specimen #2 are given in Figure 3.19 and Figure 3.20, based on the experimental values, for TEC 2007 and ASCE/SEI 41-06's limits, respectively.

During D2, the experimental values predicted all 1st storey column bottom ends to be in the SD performance level, with the top ends being in the MD performance level using TEC 2007's strain limits (Figure 3.19). The 2nd storey included a mix of member ends in the MD and SD performance level.

For ASCE/SEI 41-06's assessment, almost all 1st storey column bottom ends were predicted to be in the CP performance level, with other member ends in the specimen to be in the MD performance level (Figure 3.20). This is due to the fact that ASCE/SEI 41-06 has no tolerance for columns which have lap splice deficiencies. Once the member end rotates past the yield value, it is immediately classified as being in the CP performance level. Therefore, ASCE/SEI 41-06's rotation-based assessment is overly conservative in this regard and gives a poor prediction, as the physical specimen was still in relatively good condition after this ground motion.

Another contributing factor to this over-estimation could have been that a soft-storey mechanism was predicted in the time history analyses, which was not observed in the physical test. As mentioned before, the lack of a more detailed joint model which could properly redistribute damage could have led to the accumulation of damage in the 1st storey columns and these incorrect predictions.

Figure 3.21 shows the conditions of two 1st storey columns during D2. It is clear that the damages do not meet the requirements of being in a CP performance level.

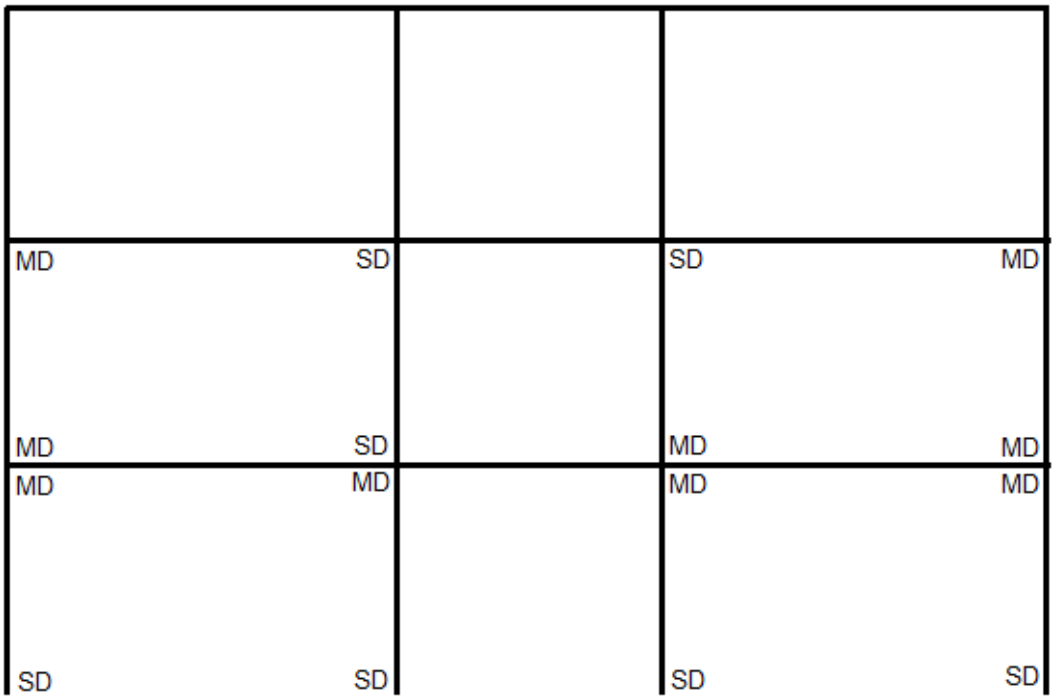

Figure 3. 19 Specimen #2 performance evaluation w.r.t. TEC damage state levels (experimental peak demands)

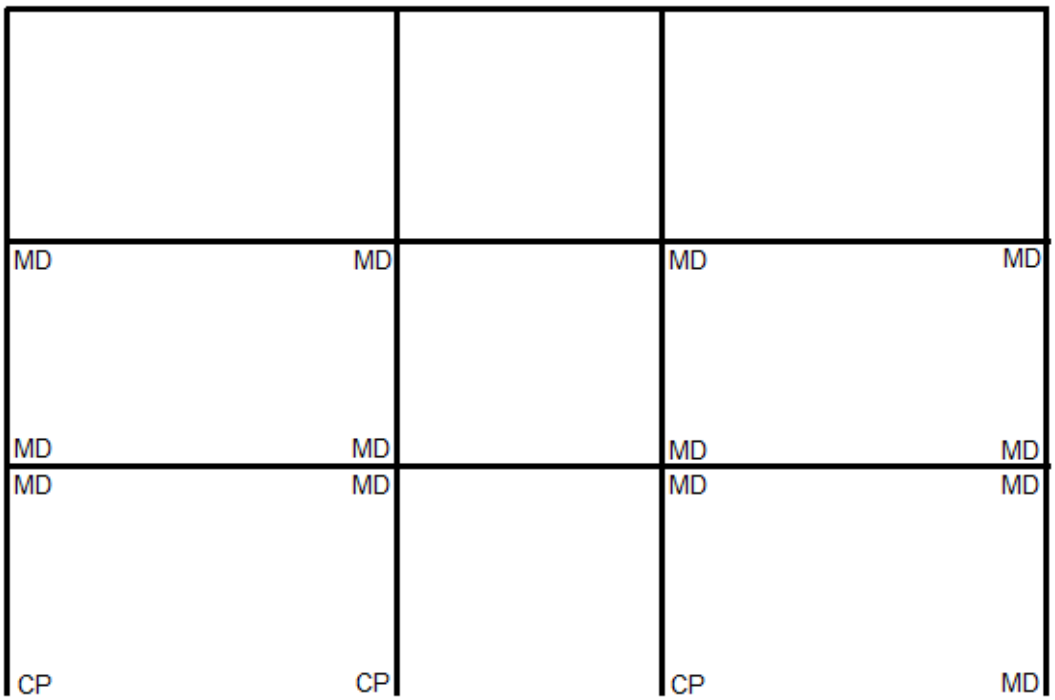

Figure 3. 20 Specimen #2 performance evaluation w.r.t. ASCE performance levels (experimental peak demands)

Figure 3. 21 Specimen #2 1st storey column damages during D2

Performance evaluations of Specimen #2 are given in Figure 3.22, which are based on the time history results, for TEC 2007's damage state limits using TEC 2007's deficient lap splice definition. Performance evaluations of Specimen #2 are given in Figure 3.23, which are based on the time history results, for ASCE/SEI 41-06's performance limits using ASCE/SEI 41-06's deficient lap splice definition.

Under D2, all column ends except about half the 1st storey column ends were predicted to be in the MD performance level through time history evaluations with TEC 2007's strain limits (Figure 3.22). The other 1st storey column ends were predicted to be in the SD performance level. During this ground motion in the physical test, minimal residual displacements were observed in the system due to the addition of lap splices.

Due to the fact that ASCE/SEI 41-06 has no tolerance for post yield rotations, almost all column ends in the 1st and 2nd storey were predicted to be in the CP performance level (Figure 3.23).

During this ground motion in the physical test, flexural macro-cracks were also present at the 1st storey columns and experimental results indicate that inelastic deformations occurred in the frame. The damage at the 1st storey columns during this ground motion was not significant enough to qualify the member ends to be in such an extreme performance level. Therefore, the assessment using ASCE/SEI 41-06's limits over-estimates the damages and is in general, more conservative than what was observed in the test.

It is important to note once again the there is virtually no difference in the direct output results between modelling through TEC 2007 or ASCE/SEI 41-06's lap splice definition.

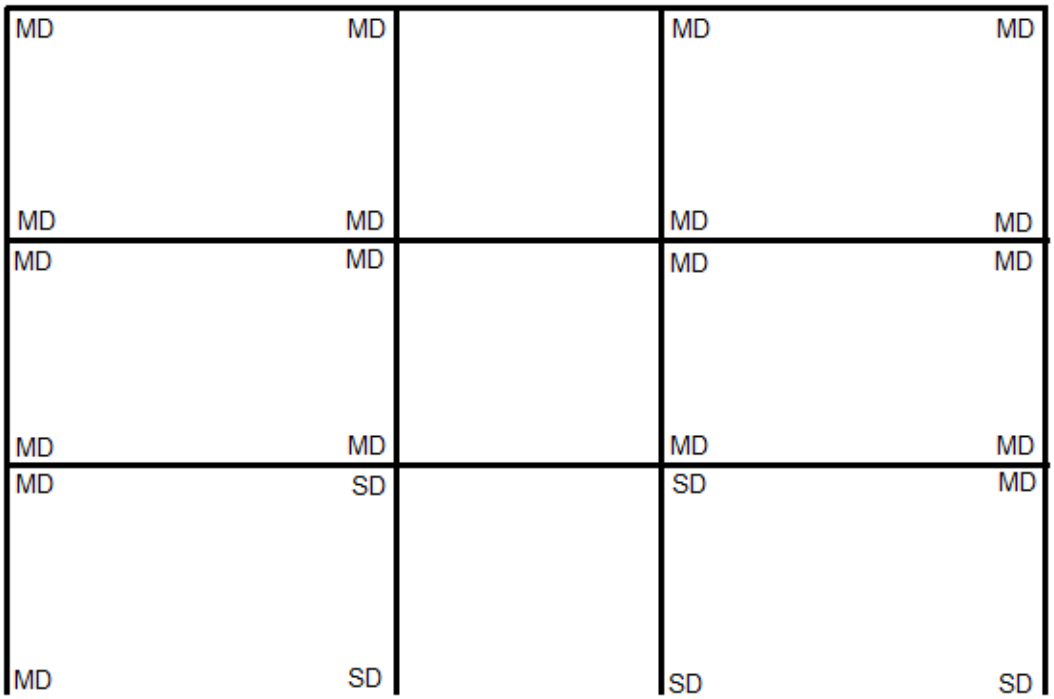

Figure 3. 22 Specimen #2 performance evaluation w.r.t. TEC damage state levels (time history peak demands, TEC splices)

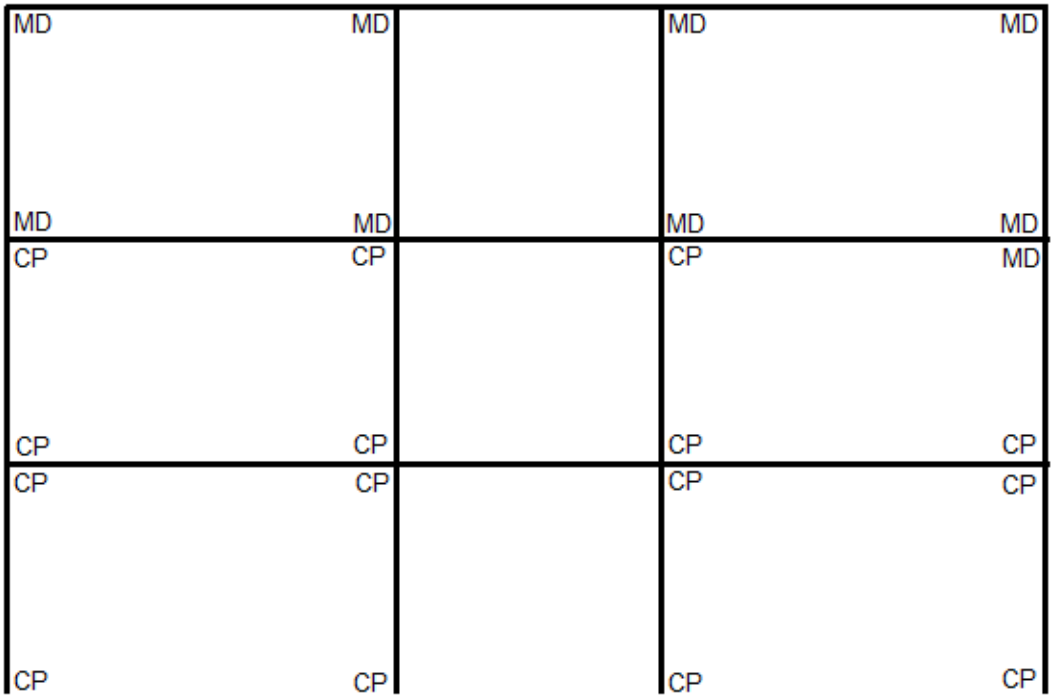

Figure 3. 23 Specimen #2 performance evaluation w.r.t. ASCE performance levels (time history peak demands, ASCE splices)

Once again, pushover analysis evaluations were not done for the ASCE/SEI 41-06 splice definition due to the fact that the OpenSees model did not capture enough of the post-peak behaviour in the capacity curves. As mentioned before, modelling materials in deficient systems by using nominal but reduced strength properties in hopes to predict accurate seismic responses is not very efficient; the inability of capturing the degradation behaviour renders pushover analysis performance evaluations impossible. The capacity curves and demands for Specimen #2's TEC 2007 and ASCE/SEI 41-06's splice models are shown in Figure 3.24 and Figure 3.25, respectively. Figure 3.26 presents the capacity curves superimposed on to the base shear vs. roof displacement plots from the experiments. Up until the points of instabilities in the models, the capacity curves capture the values recorded during the experiments rather well. It is generally accepted that pushover analysis, which is easier to implement than time history analysis, yields more conservative results as there is a trade-off between simplicity and accuracy.

It should be reiterated that damages observed during D2 for this specimen did not justify the classification of member ends to be in the CP performance level predicted in ASCE/SEI 41-06's performance assessments. A 25% lap splice length deficiency did not seem to be as detrimental to the specimen as what ASCE/SEI 41-06's assessments estimated them to be.

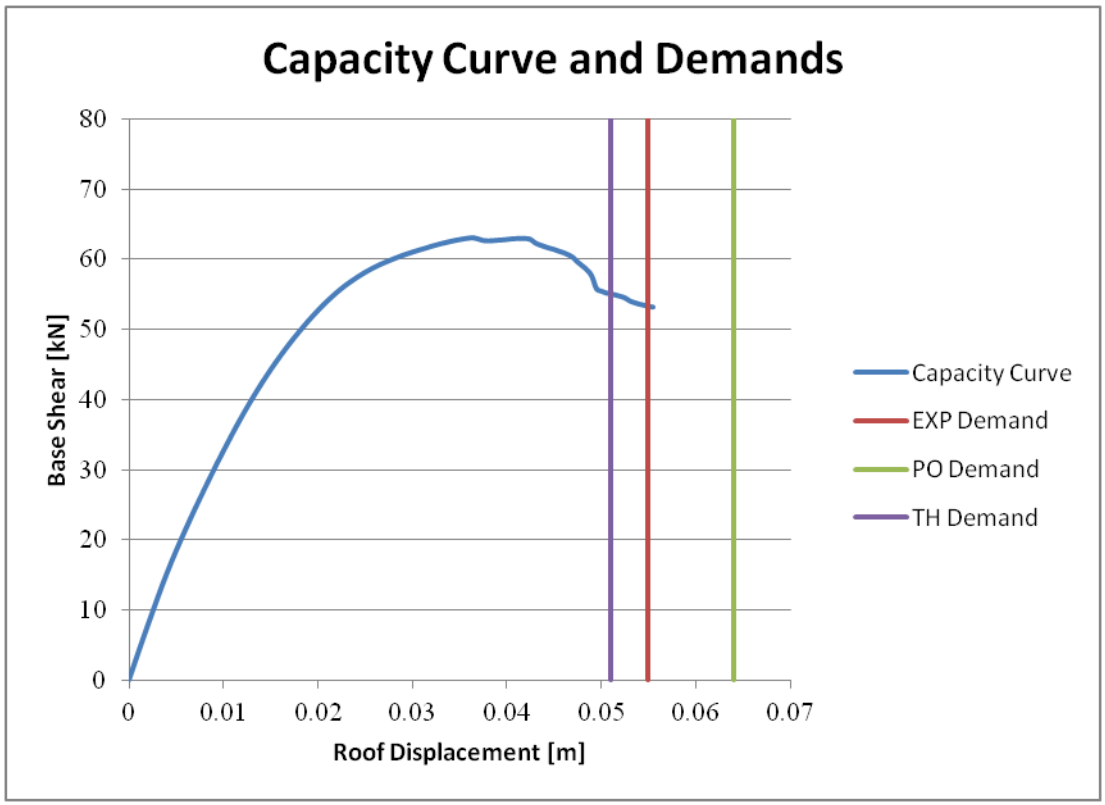

Figure 3. 24 Specimen #2 capacity curve and demands (TEC splices)

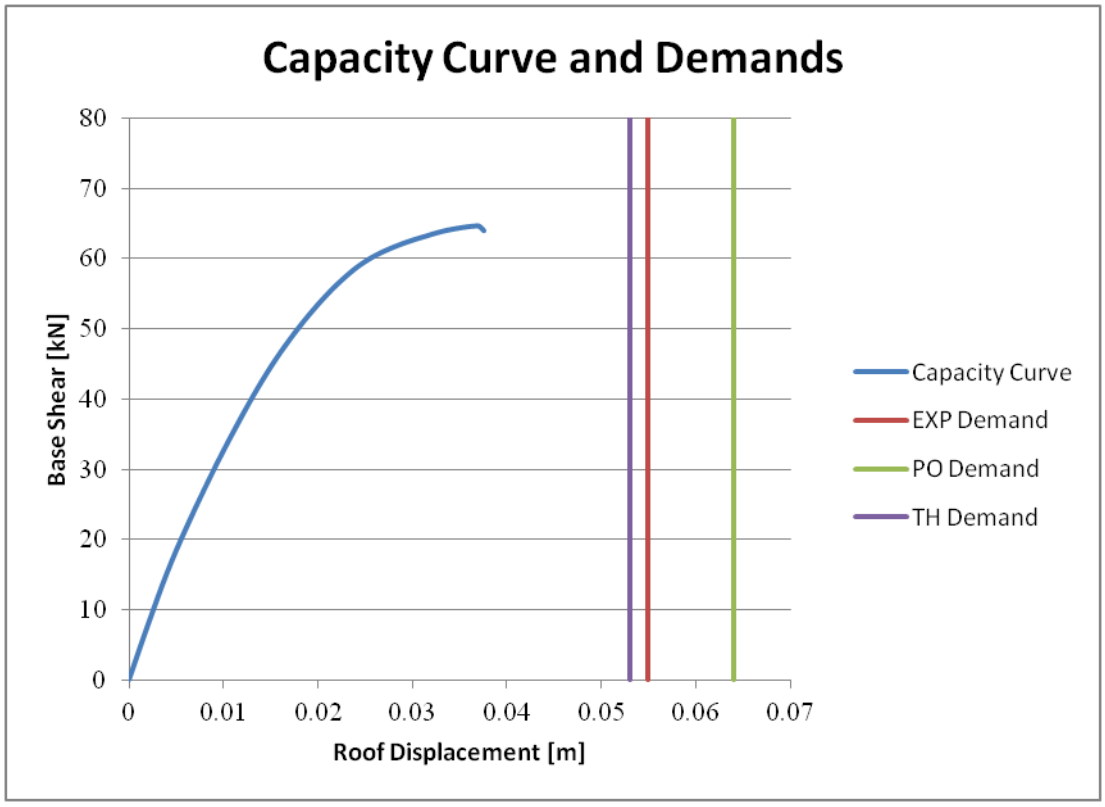

Figure 3. 25 Specimen #2 capacity curve and demands (ASCE splices)

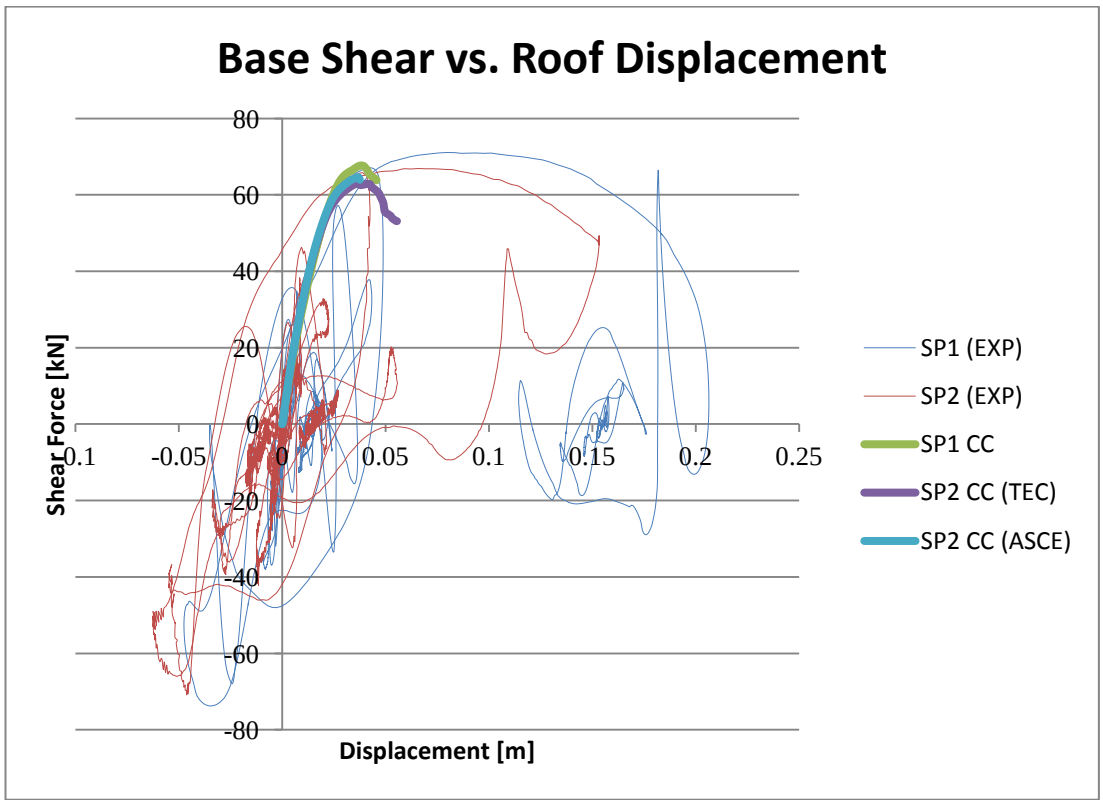

Figure 3. 26 Base shear vs. roof displacement responses and capacity curves

3.6.4 Discussion

As the OpenSees model was more reliable for the 1st storey, Table 3.11 compares the performance levels at the 1st storey column member ends during D2 for the experimental values, time history values, and what was observed in Specimen #1.

Table 3. 11 Specimen #1 1st storey column performance levels

	Column 101		Column 102		Column 103		Column 104	
	Bot.	Top	Bot.	Top	Bot.	Top	Bot.	Top
EXP (TEC)	SD	MD	SD	MD	SD	MD	SD	MD
EXP (ASCE)	MD	MD	MD	MD	MD	MD	MD	MD
TH (TEC)	MD	MD	SD	SD	SD	MD	SD	MD
TH (ASCE)	SD	MD	SD	MD	SD	SD	SD	MD
Observation	SD	MD	SD	MD	SD	MD	SD	MD

In Specimen #1, the only assessment which was less conservative was ASCE/SEI 41-06's assessment using the experimental values. This assessment predicted all column member ends to be in the MD performance level. The other three assessments predicted similar column member ends in the 1st storey to be in the SD performance level, which was more representative of the observations.

In the experiment during D2, no inclined cracks were observed. Larger than hairline flexural cracks were observed at the 1st storey column bottom ends, but it is expected that when using plain reinforcing steel, relatively larger cracks will be observed due to the lack of a physical bond between the concrete and steel. No crushing of concrete cover was observed throughout this ground motion. Even though there was a permanent drift, which indicates permanent damages were experienced, cracks were not very visible upon completion of D2. Therefore, all 1st storey column bottom ends in the experiment after D2 were in the SD performance level with the top ends being in the MD performance level. All assessments except for ASCE/SEI 41-06's experimental value assessment were reasonable representations.

Table 3.12 shows the performance levels at the 1st storey column member ends after D2 for the experimental values, time history values, and what was observed in Specimen #2.

Table 3. 12 Specimen #2 1st storey column performance levels

	Column 101		Column 102		Column 103		Column 104	
	Bot.	Top	Bot.	Top	Bot.	Top	Bot.	Top
EXP (TEC)	SD	MD	SD	MD	SD	MD	SD	MD
EXP (ASCE)	CP	MD	CP	MD	CP	MD	MD	MD
TH (TEC)	MD	MD	SD	SD	SD	SD	SD	MD
TH (ASCE)	CP	CP	CP	CP	CP	CP	CP	CP
Observation	MD	MD	MD	MD	MD	MD	MD	MD

In Specimen #2, TEC 2007's assessments were less conservative than ASCE/SEI 41-06's assessments. TEC 2007 once again predicted similar column member ends in the 1st storey to be in the SD performance level for the respective TEC 2007 experimental and time history assessments. ASCE/SEI 41-06 predicted almost half of the column ends to be in the CP performance level for the experimental value assessment. ASCE/SEI 41-06's time history assessment predicted all 1st storey column member ends to be in the CP performance level.

In the experiment during D2, no inclined cracks were observed. Cracks were observed, but in slightly lesser quantities compared to Specimen #1. Once again, no crushing of concrete cover was observed throughout this ground motion. There was almost no permanent drift, indicating that any permanent damages experienced were less than those experienced by Specimen #1. Reinforcement pullout was not observed during D2. Cracks were not very visible upon completion of the ground motion compared to the cracks observed in Specimen #1. Therefore, all columns in the experiment after D2 are in the MD performance level, making TEC 2007's assessments slightly conservative, and ASCE/SEI 41-06's assessments overly conservative.

The extreme predictions in ASCE/SEI 41-06's assessments can be attributed to two reasons: the different definitions for the reduction in reinforcing steel yield strength in the model, and as mentioned before, the lack of tolerance for column member end rotations which have gone past the yield value.

4. CONCLUSIONS

4.1 General

Results of pseudo-dynamic tests on two 3-storey, 3-bay deficient concrete frames and their respective mathematical modelling results were presented in this thesis. Numerical models in OpenSees were created to simulate the results of the pseudo-dynamics tests and calibrated in terms of the global response parameters. This study focused on the effects of insufficient lap splices on the physical frames and the comparison of methods suggested in TEC 2007 and ASCE/SEI 41-06 to account for this deficiency. Global and local forces and deformations predicted by these models were examined and performance evaluations were conducted according to nonlinear procedures in TEC 2007 and ASCE/SEI 41-06.

As the model during the intermediate ground motion was comparatively more reliable, illustrative comparisons of these results were presented. The damages observed and experimental strain assessments matched the performance levels estimated through the procedure outlined in TEC 2007 rather well for both specimens with regards to time history analysis performance evaluations, justifying the use of this procedure.

Specific to the specimen with lap splice deficiencies, the lack of tolerance beyond the yield rotation experienced by a column as defined in ASCE/SEI 41-06 lead to overly conservative results for the time history assessments. The assessment using experimental values also predicted overly conservative performance level at column ends. Damages observed did not justify the classification of member ends to be in such extreme performance level. A 25% lap splice length deficiency did not seem to be as detrimental to the specimen as what ASCE/SEI 41-06's assessments estimated them to be.

Furthermore, the presence of 25% deficient lap splice lengths in the laboratory for the second specimen did not affect the overall response, or change the failure mode when compared to the first specimen. Therefore, TEC 2007's requirements for lap splice lengths can be seen as quite conservative and are able to tolerate deficiencies up to 25% of the required length. Also, at both the global and local scale, it appears that TEC 2007 and ASCE/SEI 41-06's definition to account for lap splices did not yield significantly different modelling results.

Modelling materials in deficient systems by using nominal but reduced strength properties in hopes to predict accurate seismic responses was not very efficient in the OpenSees models. The main cause was the inability of modelling degradation during the ground motions. In addition to this, another observation was that unless joint deformations are explicitly accounted for, local deformations such as end rotations cannot be captured. In general, estimating seismic responses on a local scale is an extremely challenging, if not impossible, task.

REFERENCES

Akin, E., "Strengthening of Brick Infilled RC Frames with CFRP Reinforcement-General Principles", Dissertation Middle East Technical University, 2011. Print.

American Society of Civil Engineers, "Seismic Rehabilitation of Existing Buildings", *ASCE/SEI 41*, Reston, Virginia, 2007.

American Society of Civil Engineers, "Seismic Rehabilitation of Existing Buildings: Supplement #1", *ASCE/SEI 41*, Reston, Virginia, 2007.

Aboutaha, R.S., Engelhardt, M.D., Jirsa, J.O. and Kerger, M.E., "Retrofit of Concrete Columns with Inadequate Lap Splices by the Use of Rectangular Steel Jackets", *Earthquake Spectra*, Vol. 12, No. 4, Nov. 1996, pp. 693-714.

Binici, B. and Mosalam, K.M., "Analysis of Reinforced Concrete Columns Retrofitted with Fiber Reinforced Polymer Lamina", *Composites: Part B*, Vol. 38, pp. 265-276, 2007.

Birely, A. C., Lowes, L. N., and Lehman, D. E., "Linear Analysis of Concrete Frames Considering Joint Flexibility", *ACI Structural Journal*, Vol. 109, No. 3, May-June 2012.

Canbay, E., Ersoy, U., Ozcebe, G., "Contribution of Reinforced Concrete Infills to Seismic Behavior of Structural Systems", *ACI Structural Journal*, Vol. 100, No. 5, pp. 637-643, September 2003.

Coleman, J. and Spacone, E., "Localization Issues in Force-Based Frame Elements", *Journal of Structural Engineering*, ASCE, Vol. 127, No. 11, pp. 1257-1265, 2001.

Chopra, A.K. and Goel R.K., "A Modal Pushover Analysis Procedure for Estimating Seismic Demands for Buildings", *Earthquake Engineering and Structural Dynamics*, Vol. 31, 2002, pp. 561-582.

Dazio, A. and Yazgan, U., "Simulating Maximum and Residual Displacements of RC Structures", *Earthquake Spectra*, Vol. 27, No. 4, Nov. 2011, pp. 1182-1218.

EERI/PEER, "New Information on the Seismic Performance of Existing Concrete Buildings",*Seminar Notes*, Earthquake Engineering Research Institute, Oakland, California, 2006.

Eligehausen, R., Popov, E.P., and Bertero, V.V., "Local Bond Stress-Slip Relationships of Deformed Bars, under Generalized Excitation", *Report* UCB/EERC-83/23, Berkeley, EERC, University of California, U.S.A., 1983.

Eshghi, S. and Zanjanizadeh, V., "Cyclic Behavior of Slender R/C Columns with Insufficient Lap Splice Length", *The 14th World Converence on Earthquake Engineering*, Beijing, China, October 12-17, 2008.

Federal Emergency Management Agency, "Guidelines for the Seismic Rehabilitation of Buildings", *Report* No. FEMA-273, Oct. 1997.

Federal Emergency Management Agency, "Prestandard and Commentary for the Seismic Rehabilitation of Buildings", *FEMA (Series) 356*, Federal Emergency Management Agency, Washington, D.C., 2000.

Ghobarah A., Aziz T., And Abou-Elfath H., "Softening Effect on the Seismic Response of Non-Ductile Concrete Frames", *Journal of Earthquake Engineering*, Vol. 3, No. 1, 1999, pp. 59-81.

Harajli, M.H., “Development/Splice Strength of Reinforcing Bars Embedded in Plain and Fiber Reinforced Concrete”, *ACI Structural Journal,* Vol. 91, No. 5, September-October 1994, pp. 511-520.

Karsan, I.D., and Jirsa, J.O., “Behavior of Concrete under Compressive Loading.*” Journal of Structural Division*, ASCE, Vol. 95, No. ST12, 1969, pp. 2543-2563.

Kent, D. C., and Park R., "Flexural Members with Confined Concrete," *Journal of the Structural Division*, ASCE, Vol. 97, No. ST7, July 1971, pp. 1969-1990.

Lynn, A. C., Moehle, J. P., Mahin, S. A., and Holmes, W. T., “Seismic Evaluation of Existing Reinforced Concrete Building Columns”, *Earthquake Spectra*, Vol. 12, No. 4, Nov. 1996, pp. 715-739.

Mahin, S. A., and Shing, P. B., “Pseudodynamic Method for Seismic Testing”, *Journal of Structural Engineering*, ASCE, Vol. 111, No. 7, pp. 1482-1503, 1985.

Mazzoni et al., “OpenSees Command Language Manual”, *Pacific Earthquake Engineering Research Center*, 2007.

Melek, M. and Wallace, J.W., “Cyclic Behavior of Columns with Short Lap Splices”, *ACI Structural Journal*, Vol. 101, No. 6, 2004, pp. 802-811.

Middle East Technical University. “108G084 Tübitak Project Progress Report #1”. Aug. 5, 2010.

Molina, F. J., Pegon, P., and Verzeletti, G. “Time-domain identification from seismic pseudodynamic test results on civil engineering specimens”, *2nd International Conference on Identification in Engineering Systems*, Cromwell Press, Wiltshire, UK, 1999.

Mutlu, M.B., “Numerical Simulations of Reinforced Concrete Frames Tested using Pseudo-Dynamic Method”, Thesis Middle East Technical University, 2012. Print.

Nakashima, M., “Part 1: Relationship between Integration Time Interval and Response Stability in Pseudo Dynamic Testing”, *Journal of Structural and Construction Engineering*, Transactions of AIJ, No. 353, pp. 29-34, 1985.

Orangun, C.O., Jirsa, J.O., and Breen, J.E., “A Re-Evaluation of Test Data on Development Length and Splices”, *ACI Journal*, Vol. 74, No.3, March 1977, pp. 114-122.

Priestley, M.J.N., Ranzo, G., Benzoni, G., and Kowalsky, M.J., “Elastic Stiffness of Reinforced Concrete Bridge Columns”, *Proceedings of Fourth Caltrans Seismic Research Workshop,* July 9-11, 1996, Sacramento, California.

Sezen, H. and Moehle, J.P., “Bond-Slip Behavior of Reinforced Concrete Members”, *Proceedings of Fiber Symposium on Concrete Structures in Seismic Regions*, Greece, Athens, 2003.

Sezen, H. and Moehle, J.P., “Seismic Tests of Concrete Columns with Light Transverse Reinforcement”, *ACI Structural Journal*, Vol.103, No. 6, 2006, pp. 842-849.

Soroushian, P., Choi, K., Park, G., and Aslani, F., “Bond of Deformed bars to Concrete: Effects of Confinement and Strength of Concrete”, *ACI Materials Journal,* Vol. 88, No. 3, May-June 1991, pp. 227-232.

Takanashi, K., Udagawa, K., Seki, M., Okada, T., and Tanaka H. “Nonlinear earthquake response analysis of structures by a computer-actuator on-line system” *Bulletin of Earthquake Resistant Structure Research Center 8, Institute of Industrial Science*, University of Tokyo, Japan. 1975.

Turkish Standards Institution: Ministry of Public Works and Settlement, "Requirements for Design and Construction of Reinforced Concrete Structures", *TS 500*, Ankara, Turkey, 2000.

Turkish Standards Institution: Ministry of Public Works and Settlement, "Turkish Earthquake Code 2007", *TEC 2007*, Ankara, Turkey, 2007.

Xiao, Y. and Ma, R., "Seismic Retrofit of RC Circular Columns using Prefabricated Composite Jacketing", *Journal of Structural Engineering ASCE*, Vol. 123, No. 10, 1997, pp. 1357-1364.

Xu, Y.L., "Experimental Study of Bond-Anchorage Properties for Deformed Bars in Concrete", *Proceedings of the International Conference on Bond in Concrete*, Riga, Latvia, October 15-17, 1992.

Zhao, J. and Sritharan, S., "Nonlinear Analysis of the RC Structures with Strain Penetration Effect", *8th National Conference on Earthquake Engineering*, San Francisco, CA, U.S.A., 2006.